Pure appl. geophys. 158 (2001) 759–797
0033–4553/01/040759–39 $ 1.50 + 0.20/0

Pure and Applied Geophysics

Tsunami Excitation by Submarine Slides in Shallow-water Approximation

Stefano Tinti,[1] Elisabetta Bortolucci[1] and Cinzia Chiavettieri[1]

Abstract — Landslide-induced tsunamis are receiving increased attention since there is evidence that recent large devastating events have been caused by underwater mass failures. Normally, numerical models are used to simulate tsunami excitation, most of which are based on shallow water, known also as long wave, approximation to the full equations of hydrodynamics. Analytical studies may handle only simplified problems, but help understand the basic features of physical processes. This paper is an analytical investigation of long-water waves excited by rigid bodies sliding on the sea bottom, based on the shallow-water approximation, which is here derived by properly scaling Euler equations for an inviscid, incompressible and irrotational ocean. In one-dimensional (1-D) cases (where motion depends only on one horizontal coordinate), under the further assumptions of small-height slide, which permits the recourse to linear theory, and of flat ocean floor, a solution for arbitrary body shape and velocity is deduced by applying the Duhamel theorem. It is also shown that this theorem can be advantageously used to obtain a general solution in case of a non-flat ocean floor, when the sea bottom follows a special power law, that can be adapted to study reasonable bottom profiles. The characteristics of the excited tsunamis are then evaluated by computing solutions in numerous examples, with special focus on wave pattern and wave evolution. The energy of the wave system is shown to depend on time: it grows expectedly in the initial phase of tsunami generation, when the moving body transfers energy to the water, but it may also diminish later, implying that a certain amount of energy may pass back from water waves to the slide.

Key words: Duhamel solution, Froude number, shallow-water approximation, tsunami, underwater landslides.

Introduction

According to most tsunami catalogues, tsunamis are mostly generated by submarine earthquakes, and only a small fraction is due to slides or rockfalls. However, there is an increasing recognition that the tsunami potential of landslides may have been underestimated, and tsunamis essentially or mainly due to landslides may have been erroneously attributed to other causes. Difficulty in identifying parent mass failures in tsunami generation is understandable for historical events, whose description relies exclusively upon accounts of eyewitnesses: for example, if an

[1] Dipartimento di Fisica, Settore di Geofisica, Università di Bologna, Viale Carlo Berti Pichat, 8, 40127 Bologna, Italy.

earthquake sets in motion a submarine slump that in turn produces a tsunami that attacks a nearby coastline, the coastal population may tend to relate the tsunami to the seismic shock, since in general underwater slumps pass unobserved. But there may be difficulties even for recent occurrences, as demonstrated by the case of the catastrophic tsunami that struck the north coast of Papua New Guinea on the evening of 17 July 1998, causing more than 2200 fatalities (DAVIES, 1999; KAWATA *et al.*, 1999). Intensive research and data analysis have not yet provided a definite answer on the origin of the tsunami (was it due directly to a submarine earthquake that produced a dislocation at the sea bottom or to a submarine slump triggered by the seismic sequence?), though a slump seems the favourite candidate (TAPPIN *et al.*, 1999).

Landslides in coastal areas and in the sea are known to have a large tsunami potential, depending mostly on the size of involved mass and on the slope of the sea bottom. They may originate by pure gravitational loading and instability, or they may be triggered by earthquake vibrations, or they may be associated with volcanic eruptions, mostly of the explosive type (MURTY, 1977; HAMPTON *et al.*, 1996; see also CALVARI and THANNER, 1999 for the recent onshore and offshore geological evidence for a large 10-ka seaward flank collapse of Etna volcano, with possible generation of a large tsunami). They may produce incredibly large waves that climb coastal slopes with astonishing runup of several hundred meters: very famous is the case of Lituya Bay, Alaska, where in 1958 the splashing of a huge volume of rocks generated a wave in the inlet that attacked the opposite coast and destroyed all vegetation up to the height of 500 m (MILLER, 1960; MURTY, 1977). Studies of landslide-induced tsunamis generally are based on numerical simulations. Most make use of the two-dimensional nonlinear shallow-water approximation with variables independent of the vertical coordinate z (RANEY and BUTLER, 1975; HARBITZ, 1992; JIANG and LEBLOND, 1993; IMAMURA and GICA, 1996; JOHNSGARD and PEDERSEN, 1996; FINE *et al.*, 1999; TINTI *et al.*, 1999a and 1999b), or of the 2-D linear potential theory with variables computed on vertical cross sections and uniform along one horizontal coordinate, say y (GRILLI and WATTS, 1999). Full 3-D models are rarely used because they are computationally intensive (ASSIER RZADKIEWICZ *et al.*, 1997), and when used for simulations of real tsunamis, they are mostly limited to the generation phase, with propagation computed through more economic shallow-water models (HEINRICH *et al.*, 1999). Analytical studies cannot address realistic cases with complications that derive from the geometrical complexity of the ocean basin and of the landslide, and from complex interaction between the sliding body and fluid, such as turbulence, chaotic vorticity, fluid incorporation in the sliding material, etc. These studies, however, serve to elucidate basic features of the phenomenon and to gain an understanding of physical processes, and have often been used in conjunction with laboratory experiments in hydraulic tanks with waves excited under controlled conditions (TAKAHASHI, 1943, 1948; WIEGEL, 1955; SELLS, 1965; KAJIURA, 1970; NODA, 1970, 1971; IWASAKI, 1982; SABATIER, 1983; PELINOVSKY and POPLAVSKY, 1996; WATTS, 1998).

In this paper we use analytical means to study tsunami generation by submerged sliding masses, using the approximation of shallow water or long waves. First, shallow-water equations in the case of the elevation of the ocean bottom changing with time (which is the assumption needed to describe a moving mass) will be rigorously deduced by applying a scaling method based on power expansions, that was successfully applied by FRIEDRICHS (1948) and by STOKER (1957). Scaling, which is a technique that enables the assessment of the appropriate weight of any term in a set of differential equations, has been often applied to Euler or to Navier-Stokes equations that govern the motion of a fluid to work out meaningful approximations (see PEREGRINE, 1972; HAMMACK, 1973; ICHIYE, 1983; VILLENEUVE and SAVAGE, 1993; WATTS, 1998). With our approach we highlight the conditions under which the shallow-water approximation holds in case of landslide-induced tsunamis. We study the shallow-water approximation for 1-D linear problems in an ocean of constant depth, and use the Duhamel theorem to deduce an explicit form of the solution that describes water waves excited by bodies of any shape and arbitrary velocity, which generalises formulas and results obtained in previous investigations on slides that move with constant velocity (HARBITZ and ELVERHØI, 1999; TINTI and BORTOLUCCI, 2000a). Furthermore, we also study tsunami generation in the case of a non-flat ocean bottom, since it will be shown that, when depth follows a special power law, the problem may be reduced to a corresponding flat-bottom case through an appropriate coordinate transformation and admits therefore an explicit solution in view of the Duhamel theorem. The main characteristics of the engendered tsunamis are examined and discussed by numerous cases. Special attention is given to the shape, amplitude and celerity of the waves and to the energy that is exchanged between the body and the water. It will be seen that tsunami generation requires a net transfer of energy from the body to the sea, since the former is the source of the water waves, although there may be phases of the interaction process during which energy transfer takes place in the other way, and waves tend to loose energy with time.

Formulation of the Problem

Tsunami generation and evolution may be studied by means of the equations that govern the motion of a fluid. Under the assumptions that the water is incompressible and inviscid, and if it is further required that no turbulent nor chaotic motions can take place within the fluid, the classical Euler equations of hydrodynamics can be used. In a Cartesian reference frame, let us take the plane x, y to be the horizontal free surface of the water in still conditions, that is the mean-sea-level (msl) surface, and the z axis be vertically upward, with the origin placed on the msl surface. The sea surface and the basin bottom at any time t are respectively described by the equations:

$$z_s = \xi(x, y, t), \tag{1}$$

$$z_b = -h^*(x, y, t), \tag{2}$$

where $\xi(x, y, t)$ is the instantaneous water elevation measured from the msl. In dealing with water waves excited by an underwater mass, it is convenient to assume that the instantaneous basin depth $h^*(x, y, t)$ has the form:

$$h^*(x, y, t) = h(x, y) - h_s(x, y, t), \tag{3}$$

where $h_s(x, y, t)$ is the submarine sliding mass with height depending on space and time, and $h(x, y)$ is the basin depth in still conditions, with no dependence on time. With these assumptions positive values of h_s are adequate to describe uplift of the ocean floor or a submarine mass sliding along the sea floor, whereas negative values would depict subsidence (see sketch of Fig. 1).

If the velocity components of the water particles along the axes x, y and z are designated respectively by u, v, w, and if water pressure is denoted by p, the full set of nonlinear hydrodynamic equations can be written as follows (STOKER, 1957):

$$u_x + v_y + w_z = 0, \tag{4.1}$$

$$u_t + uu_x + vu_y + wu_z = -\frac{1}{\rho} p_x, \tag{4.2}$$

$$v_t + uv_x + vv_y + wv_z = -\frac{1}{\rho} p_y, \tag{4.3}$$

$$w_t + uw_x + vw_y + ww_z = -\frac{1}{\rho} p_z - g, \tag{4.4}$$

$$w_y = v_z \quad u_z = w_x \quad v_x = u_y. \tag{4.5}$$

Here ρ and g respectively denote water density and vertical component of gravitational acceleration, and are taken to be constant in this analysis. Notice also

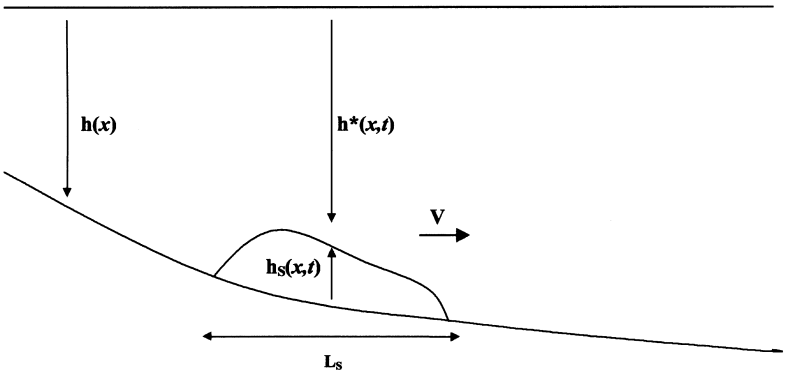

Figure 1
Schematic drawing of the landslide with notation used in the paper.

that use is made of subscripts to denote partial differentiation with respect to the subscripted variable. Condition (4.1) stating that the fluid divergence is identically zero is the expression of the continuity equation in case of constant-density fluids. Equations (4.2)–(4.4) are the momentum equations, and finally the set of eqs. (4.5) express the condition of irrotational flow, that is adequate for fluids that are supposed to be initially at rest, and consequently to possess no initial vorticity, due to vorticity conservation. The above system of equations must be fulfilled within the volume $\Omega(x, y, z, t)$ which is defined by:

$$x, y \in \Omega_{\mathrm{h}}(x, y, z, t) \tag{5.1}$$

$$z_b \leq z \leq z_s, \text{ i.e. } -h^*(x, y, t) \leq z \leq \xi(x, y, t) \tag{5.2}$$

where $\Omega_{\mathrm{h}}(x, y, z, t)$ is the projection of Ω on the horizontal plane x, y. This definition of Ω_{h} covers cases where the basin is limited by vertical walls, as well as cases where boundaries are slopes with complex profile. It is worth noticing that in general the domain Ω changes dynamically with the water motion, both along the vertical axis z, as well as on the horizontal plane x, y. If Ω is a domain of finite extension, this implies that Ω_{h} is a finite plane surface. Its boundary may be either artificial lines delimiting the basin at the open sea or the instantaneous basin shoreline, and may change with time in consequence of flows and ebbs associated with water waves. The unknowns of the system formed by eqs. (4) within the domain Ω given by relationships (5) are the velocity components u, v and w, the pressure field p and the water elevation ξ. The system must be complemented by initial conditions and by boundary conditions. If the fluid is initially at rest with null velocity and null elevation, then hydrostatic equilibrium holds, and initial conditions assume the form:

$$u(x, y, z, 0) = v(x, y, z, 0) = w(x, y, z, 0) = \xi(x, y, 0) = 0 \tag{6.1}$$

$$p(x, y, z, 0) = -\rho g z + p_0 \tag{6.2}$$

where p_0 is the pressure initially exerted by the atmosphere on the sea surface, and is a constant value. The conditions on the upper and bottom surfaces of the fluid can be imposed by assuming that they are material surfaces, viz. formed by the same particles of fluid at any time, and in addition, by specifying the atmospheric pressure forcing. The consequent equations are:

$$\xi_t + u\xi_x + v\xi_y - w = 0 \quad \text{at } z = z_s = \xi(x, y, t), \tag{7.1}$$

$$p = p(x, y, t) \quad \text{at } z = z_s = \xi(x, y, t), \tag{7.2}$$

$$uh_x + vh_y + w = \partial_t h_s \quad \text{at } z = z_b = -h^*(x, y, t). \tag{7.3}$$

Notice that, to avoid confusion, partial differentiation of the function h_s with respect to time is denoted by the symbol ∂_t in place of the subscript t. Compatibility between eqs. (6) and (7) implies that atmospheric pressure be initially constant over the basin, namely $p(x, y, 0) = p_0 = \text{constant}$. Owing to the purposes of the present study which

is focussed on waves produced not through sea-surface forcing but by underwater sources, we will impose the even more drastic requirement that atmospheric pressure is negligibly small, that is:

$$p(x, y, t) = p_0 = 0. \tag{7.4}$$

Notwithstanding the simplifications implied by the assumptions we made in the formulation, which rule out important phenomena such as wave excitation by atmospheric wind stresses at the sea surface, the problem mathematically described by the above equations (1)–(7) covers a large variety of processes, such as generation of waves forced by moving portions of basin boundaries (which is the most common way to produce water waves in laboratory experiments where sectors of boundaries – upper, lower or lateral – are mechanically moved with prescribed time histories), tsunamis induced by earthquakes and by landslides, and propagation of waves that enter the basin through lateral open boundaries. Nevertheless, this system of equations presents mathematical difficulties and cannot be solved analytically unless further approximations are introduced. One of the most relevant approximations concentrates on waves with typical horizontal scale large compared to the typical water depth, and is known as long-wave theory or, equivalently, as shallow-water approximation.

Shallow-water Approximation

Shallow-water theory will be derived here from the full set of Euler equations, by applying a modified version of the method used by STOKER (1957) who took into account the particular case of a basin with a steady sea floor, viz. with bottom surface not dependent on time ($z_b = -h^*(x, y)$), and who therefore excluded the case of landslide generation that is of most interest in this paper. The method is based on expanding all quantities in series of powers of a small parameter, $\varepsilon \ll 1$, and on obtaining new sets of equations by equating all terms corresponding to the same powers of ε. This procedure provides one system of equations for any one power of the parameter, and in order to be workable in practice, it requires truncation to a certain order. Shallow-water theory is the approximation resulting from truncating the process at the lowest possible order.

The first step is to provide the nondimensional version of the governing system of equations (1)–(7). This will be performed in an abbreviated way here below, while full details are given in Appendix A. Let us now introduce dimensionless variables by using three lengths, D, d and k, representing respectively the typical water depth, the typical amplitude of the bottom disturbance, namely the landslide thickness, as well as of the water elevation, and the typical horizontal distance for the water motion. This last, in our case, may represent the characteristic length of the waves as well as the characteristic length of the bottom perturbation, such as the landslide length.

From the above three lengths, two important ratios may be derived, namely the aspect ratio δ and the expansion parameter ε, according to the following definitions:

$$\delta = d/D \quad \varepsilon = D/k. \tag{8}$$

The former, being the ratio between the amplitude of the water waves and the typical ocean depth, cannot be larger than unity, whereas the latter in principle may assume any values from very small to very large. Here, however, it will be taken as a very small quantity, and on the basic hypothesis of $\varepsilon \ll 1$, the entire construction of the shallow-water theory will be built up. A characteristic speed c also may be introduced, enabling us to scale the time t through a characteristic time t_c defined as:

$$t_c = k/c \quad \text{with} \quad c = \sqrt{gD}. \tag{9}$$

From the above, t_c is the time taken by a disturbance to travel the horizontal distance k at the speed c. The reason for this choice for c will be clarified *a posteriori* when c will be shown to be the celerity of free waves in shallow water.

The new independent space-time coordinates in dimensionless form are:

$$x' = x/k \quad y' = y/k \quad z' = z/D \quad t' = t/t_c. \tag{10.1}$$

Furthermore, dimensionless velocities can be obtained as follows:

$$u' = u/(\delta c) \quad v' = v/(\delta c) \quad w' = w/(\varepsilon \delta c). \tag{10.2}$$

Finally, the remaining dimensionless unknowns p' and ξ', and the dimensionless known functions involved in the bottom-surface description, h' and h'_s, can be written as:

$$p' = p/(\rho g D) \quad \xi' = \xi/d \quad h' = h/D \quad h'_s = h_s/d. \tag{10.3}$$

Observe that horizontal quantities have been scaled differently from vertical ones, and that the pressure scale is the hydrostatic pressure value $\rho g D$.

After introducing the new dimensionless variables in the set of equations and definitions (1)–(7), the following relationships are obtained, that for the sake of simplicity are written more conveniently by dropping the primes:

$$u_x + v_y + w_z = 0, \tag{11.1}$$

$$\delta[u_t + \delta(uu_x + vu_y + wu_z)] + p_x = 0, \tag{11.2}$$

$$\delta[v_t + \delta(uv_x + vv_y + wv_z)] + p_y = 0, \tag{11.3}$$

$$\delta\varepsilon^2[w_t + \delta(uw_x + vw_y + ww_z)] + p_z + 1 = 0, \tag{11.4}$$

$$\varepsilon^2 w_y = v_z \quad u_z = \varepsilon^2 w_x \quad v_x = u_y, \tag{11.5}$$

with the conditions on the boundaries given by:

$$\xi_t + \delta u\xi_x + \delta v\xi_y = w \quad \text{at } z = \delta\xi(x, y, t), \tag{11.6}$$

$$p = 0 \quad \text{at } z = \delta\xi(x,y,t), \tag{11.7}$$

$$uh_x + vh_y + w = \partial_t h_s \quad \text{at } z = -h^*(x,y,t) = -h(x,y) + \delta h_s(x,y,t). \tag{11.8}$$

This is the basic system of dimensionless equations that is also derived in Appendix A. The following step consists of expanding all variables, including the aspect ratio δ, in series of powers of ε. Assuming that the expansion of a generic function, say f, has the form:

$$f(x,y,z,t) = \sum_0^\infty \varepsilon^k f^{(k)}(x,y,z,t). \tag{12}$$

After substituting expansions such as (12) in eqs. (11), the system of equations obtained at the lowest order, that is at zeroth order, is:

$$u_x^{(0)} + v_y^{(0)} + w_z^{(0)} = 0, \tag{13.1}$$

$$\delta^{(0)}\left(u_t^{(0)} + \delta^{(0)}u^{(0)}u_x^{(0)} + \delta^{(0)}v^{(0)}u_y^{(0)}\right) + p_x^{(0)} = 0, \tag{13.2}$$

$$\delta^{(0)}\left(v_t^{(0)} + \delta^{(0)}u^{(0)}v_x^{(0)} + \delta^{(0)}v^{(0)}v_y^{(0)}\right) + p_y^{(0)} = 0, \tag{13.3}$$

$$p_z^{(0)} + 1 = 0, \tag{13.4}$$

$$v_z^{(0)} = 0 \quad u_z^{(0)} = 0 \quad v_x^{(0)} = u_y^{(0)}, \tag{13.5}$$

$$\xi_t^{(0)} + \delta^{(0)}u^{(0)}\xi_x^{(0)} + \delta^{(0)}v^{(0)}\xi_y^{(0)} = w \quad \text{at } z = \delta^{(0)}\xi^{(0)}(x,y,t), \tag{13.6}$$

$$p^{(0)} = 0 \quad \text{at } z = \delta^{(0)}\xi^{(0)}(x,y,t), \tag{13.7}$$

$$u^{(0)}h_x^{(0)} + v^{(0)}h_y^{(0)} + w^{(0)} = \partial_t h_s^{(0)} \quad \text{at } z = -h^{(0)}(x,y) + \delta^{(0)}h_s^{(0)}(x,y,t). \tag{13.8}$$

Since the analysis will be limited to this order of truncation, it is convenient to drop the symbol $^{(0)}$ in all following elaborations. The most important results that can be straightforwardly deduced from the above zeroth-order system, are that horizontal velocities u and v do not depend upon the vertical coordinate z, whereas pressure p has a simple linear dependence. On taking into account the condition (13.7) at the upper surface, from eq. (13.4) it is easy to obtain that:

$$p(x,y,z,t) = \delta\xi(x,y,t) - z \quad -h + \delta h_s < z < \delta\xi(x,y,t) \tag{14.1}$$

which is a modified version of the hydrostatic condition, since it states that pressure at a given depth is determined by the height of the overlying water column, and entails that the horizontal pressure gradient is proportional to the gradient of the water surface elevation:

$$p_x(x,y,z,t) = \delta\xi_x(x,y,t), \tag{14.2}$$

$$p_y(x,y,z,t) = \delta\xi_y(x,y,t). \tag{14.3}$$

In virtue of eqs. (13.5), the horizontal divergence of the fluid field is independent of z, implying that the vertical velocity w grows linearly with z. From eq. (13.1) it can be deduced that:

$$w(x,y,z,t) = -[u_x(x,y,t) + v_y(x,y,t)]z + F(x,y,t) \quad -h + \delta h_s < z < \delta\xi(x,y,t), \quad (15)$$

where F is an arbitrary function that can be determined by either one of the boundary conditions (13.6) or (13.8). By making use of eq. (13.6), the expression for F results to be:

$$F(x,y,t) = \xi_t(x,y,t) + \delta[u(x,y,t)\xi(x,y,t)]_x + \delta[v(x,y,t)\xi(x,y,t)]_y. \quad (16)$$

This enables us to replace the vertical velocity w in eq. (13.8) to obtain:

$$\xi_t + [u(h - \delta h_s + \delta\xi)]_x + [v(h - \delta h_s + \delta\xi)]_y = \partial_t h_s, \quad (17.1)$$

where it is meant that none of the involved variables depend on z, but they depend only on the horizontal space coordinates and on time.

After substituting expressions (14.1) and (14.2) in the respective eqs. (13.2) and (13.3), the following equations can be obtained:

$$u_t + \delta u u_x + \delta v u_y + \xi_x = 0, \quad (17.2)$$

$$v_t + \delta u v_x + \delta v v_y + \xi_y = 0. \quad (17.3)$$

Altogether, eqs. (17) form a closed system of three differential equations in the unknowns u, v and ξ, that must be complemented by the initial conditions of still water:

$$u(x,y,0) = v(x,y,0) = \xi(x,y,0) = 0 \quad (18)$$

easily derivable from the corresponding conditions (6.1). This system is known as the shallow-water approximation of the full Euler equations. It must be completed also by proper conditions on the boundary Ω_h. For example, it may be required that waves are allowed to pass across sectors of open boundaries with no back reflections, whereas boundaries representing vertical coastlines may be presumed to cause perfect wave reflection, etc. In this study we will restrict to initial-value problems, with no interest in phenomena taking place at the basin boundaries, and therefore we will not detail this issue any further. Once the system has been solved, the remaining unknowns, viz. vertical velocity w and pressure p, can be determined univocally by means of the corresponding explicit expressions (15)–(16) and (14.1). The explicit expression for the vertical velocity may be written as:

$$w = -(u_x + v_y)z + \xi_t + \delta(u\xi)_x + \delta(v\xi)_y \quad -h + \delta h_s < z < \delta\xi. \quad (17.4)$$

The system (17) is strongly nonlinear, since all equations include terms involving cross products of the unknown functions and their first derivatives, and through the term $\partial_t h_s$ in eq. (17.1) it is adequate to describe excitation of water waves by

disturbances affecting local sea depth, such as those produced by submarine earthquake dislocations or by underwater slumps or debris avalanches. It is stressed that it was derived also by TUCK and HWANG (1972) who used it to study 1-D tsunami generation by impulsive dislocations involving the ocean floor on sloping beaches by means of an analytical approach.

All nonlinear terms of the equations of the shallow-water approximation include the aspect ratio δ. If δ is assumed to be small, or more precisely, to be at least as small as the expansion parameter ε, then expression (12) implies that the first-order term of the expansion of δ, that is $\delta^{(0)}$, is zero, and, consequently, the set of equations (17.1)–(17.3) simplifies to the linear form:

$$\xi_t + (uh)_x + (vh)_y = \partial_t h_s, \tag{19.1}$$

$$u_t + \xi_x = 0, \tag{19.2}$$

$$v_t + \xi_y = 0, \tag{19.3}$$

which is adequate to study wave generation in case of small-amplitude large-scale sea-bottom perturbations. Linearization of the explicit expressions for the vertical velocity (17.4) and the pressure engenders the further equations:

$$w = -(u_x + v_y)z + \xi_t \quad -h < z < 0, \tag{19.4}$$

$$p = -z \quad -h < z < 0. \tag{19.5}$$

The former implies that at the sea surface the vertical velocity of fluid particles identifies with the rate of change of the wave elevation, whereas the latter is the pure hydrostatic condition, stating that pressure is not affected by wave generation and propagation, and preserves its initial value at any time. In this paper we will focus our attention on linear system (19), and more specifically, on the 1-D version of it, after assuming that all quantities are independent of one of the horizontal co-ordinates, say y, which also implies that the corresponding velocity component v is identically zero. Returning to the original dimensional variables, this system may be written as:

$$\xi_t + (uh)_x = \partial_t h_s, \tag{20.1}$$

$$u_t + g\xi_x = 0, \tag{20.2}$$

$$v = 0, \tag{20.3}$$

$$w = -u_x z + \xi_t \quad -h < z < 0, \tag{20.4}$$

$$p = -\rho g z \quad -h < z < 0. \tag{20.5}$$

Despite the drastic simplifications that enabled us to transform the full system of Euler equations to the above set (20), the analysis of the solution of such system has not been exhausted in the literature and, as we will see, it may lead to interesting results in the ambit of tsunami generation by underwater masses.

Linear Slide-induced Tsunamis in a Flat-bottom Sea

In case of a basin with constant depth $h(x, y) = H$, the linear system (20) reduces to a set of differential equations with constant coefficients:

$$\xi_t + Hu_x = \partial_t h_s, \tag{21.1}$$

$$u_t + g\xi_x = 0, \tag{21.2}$$

with the remaining eqs. (20.3)–(20.5) left unchanged. Since these provide explicit expressions for the related unknowns, they no longer will be taken into account in the following analysis. The corresponding initial conditions are:

$$u(x, 0) = \xi(x, 0) = 0. \tag{21.3}$$

Reverting to nondimensional variables according to the procedure of the previous section, the above system becomes:

$$\xi_t + u_x = \partial_t h_s, \tag{22.1}$$

$$u_t + \xi_x = 0, \tag{22.2}$$

$$u(x, 0) = \xi(x, 0) = 0, \tag{22.3}$$

in terms of the new unknowns, that here are designated with the same notation, in agreement with our prior convention. System (22) may be studied in several ways. One approach consists in differentiating eq. (22.1) with respect to time t, and eq. (22.2) with respect to space x, and then in subtracting the latter equation from the former member by member. Through this elementary manipulation, the following equation is obtained for water elevation ξ:

$$\xi_{tt} - \xi_{xx} = \partial_{tt} h_s, \tag{23.1}$$

where symbol ∂_{tt} has the obvious meaning of double differentiation with respect to time. Equation (23.1) is a classical inhomogeneous hyperbolic equation governing linear waves. In its homogeneous form it is fulfilled by constant-amplitude waves travelling with unit constant celerity, which converts to constant speed $c = \sqrt{gH}$ in dimensional space. Therefore, this property provides the *a posteriori* justification for the scaling factor used in (9) to define the typical shallow-water time scale t_c. Once eq. (23.1) is solved, velocity u may be computed by integrating eq. (22.2), which in light of condition (22.3) yields:

$$u = -\int_0^t \partial_x \xi(x, \tau)\, \mathrm{d}\tau. \tag{23.2}$$

Notice that in passing from the original formulation (22), involving two unknown functions u and ξ, to problem (23), with the only unknown ξ, the system transforms from first- to second-order of differentiation. Therefore, in order to

ensure that it has a unique solution, initial conditions for both ξ and ξ_t must be provided. From conditions (22.3) it is easy to infer that u_x must be identically zero at the initial time, and thus with the aid of eq. (22.1) the following conditions may be deduced:

$$\xi(x,0) = 0, \tag{23.3}$$

$$\xi_t(x,0) = \partial_t h_s(x,0). \tag{23.4}$$

Due to the linearity of the system, its solution may be calculated as the sum of the solutions of two related problems, that is:

$$\xi(x,t) = \xi_1(x,t) + \xi_2(x,t), \tag{24}$$

where ξ_1 satisfies the homogeneous differential equation with inhomogeneous initial conditions, whereas ξ_2 satisfies the inhomogeneous differential equation with homogeneous initial conditions. The former system is of the type:

$$\xi_{tt} - \xi_{xx} = 0, \tag{25.1}$$

$$\xi(x,0) = \alpha(x) \quad \xi_t(x,0) = \beta(x). \tag{25.2}$$

This initial-value problem describes a free wave propagating from an initial configuration $\alpha(x)$ with a prescribed initial surface vertical velocity $\beta(x)$. In applications concerning tsunamis induced by earthquakes, wave evolution is often computed by means of this problem, where $\alpha(x)$ is the sea-surface displacement caused by the earthquake, taken to be similar to the ocean bottom dislocation, and $\beta(x)$ is identically zero (see e.g., AIDA, 1969; SKLARZ *et al.*, 1979; CHUBAROV *et al.*, 1984; TINTI *et al.*, 1994; TINTI and PIATANESI, A., 1996; YAMASHITA *et al.*, 1997; PIATANESI and TINTI, 1998). The general solution to the Cauchy problem (25) may be expressed in the form (ZWILLINGER, 1989):

$$\xi(x,t) = \frac{1}{2}[\alpha(x-t) + \alpha(x+t)] + \frac{1}{2}\int_{x-t}^{x+t} \beta(\chi)\,\mathrm{d}\chi \tag{25.3}$$

and, accordingly, ξ_1 results to be:

$$\xi_1(x,t) = \frac{1}{2}\int_{x-t}^{x+t} \partial_t h_s(\chi,0)\,\mathrm{d}\chi. \tag{26}$$

The second problem is:

$$\xi_{tt} - \xi_{xx} = \varphi(x,t), \tag{27.1}$$

$$\xi(x,0) = \xi_t(x,0) = 0, \tag{27.2}$$

and its solution may be found in virtue of the Duhamel theorem, by exploiting the general solution to the Cauchy problem (25). The Duhamel theorem (FOLLAND,

1995) states that, given problem (27), if the function $\gamma(x,t,q)$, depending on the dummy parameter q in addition to the space and time variables, is the solution of the associated Cauchy problem defined by:

$$\gamma_{tt} - \gamma_{xx} = 0, \tag{27.3}$$

$$\gamma(x,0,q) = 0, \tag{27.4}$$

$$\gamma_t(x,0,q) = \varphi(x,q), \tag{27.5}$$

then the searched solution to (27) is provided by the following integral:

$$\xi(x,t) = \int_0^t \gamma(x,t-q,q)\,\mathrm{d}q. \tag{27.6}$$

Bearing in mind that in our case $\varphi(x,q) = \partial_{qq}h_s(x,q)$, after combining (25.3) and (27.6), the explicit form for the solution is:

$$\xi_2(x,t) = \frac{1}{2}\int_0^t \mathrm{d}q \int_{x-(t-q)}^{x+(t-q)} \mathrm{d}\chi\ \partial_{qq}h_s(\chi,q). \tag{28}$$

To be applied, the Duhamel theorem requires that both $\varphi(x,q)$ and $\varphi_x(x,q)$ be continuous functions of the space coordinate x, which imposes equivalent continuity restrictions on $\partial_{qq}h_s(x,q)$ and on $\partial_{qqx}h_s(x,q)$. In expression (28) the integrand function $\partial_{qq}h_s(\chi,q)$ may be viewed as the source of the perturbation, the integrand variables χ and q are respectively the space and time variables associated with the source, while x and t are the independent coordinates that may be interpreted here as the coordinates of the observation point. In conclusion, the final solution to the original problem (23) is found by combining expressions (24), (26) and (28), that is:

$$\xi(x,t) = \frac{1}{2}\int_{x-t}^{x+t} \partial_t h_s(\chi,0)\,\mathrm{d}\chi + \frac{1}{2}\int_0^t \mathrm{d}q \int_{x-(t-q)}^{x+(t-q)} \mathrm{d}\chi\ \partial_{qq}h_s(\chi,q). \tag{29}$$

In this paper most of the attention is focussed on tsunami generation by submarine slides. Therefore $h_s(x,t)$ represents a mobile mass of material sliding on the stationary sea-bottom surface. If the slide undergoes negligible deformation during its motion, which is often a good first-order approximation for underwater slumps, or if it moves as a perfectly rigid body, then its motion may be univocally specified by means of the instantaneous slide velocity V(t), and of its corresponding dimensionless counterpart Fr(t), which, consistent with our previous scaling procedure, is obtained as the numeric ratio of V(t) to the wave celerity c. This ratio is known as slide Froude number and plays an important role in determining

the tsunami potential of the slide. The above considerations imply that h_s is a function of a unique argument, that is:

$$h_s(x,t) = h_s(\sigma) \quad \text{with} \quad \sigma = x - \int_0^t \mathrm{Fr}(\tau)\,\mathrm{d}\tau, \tag{30.1}$$

where the integral represents the dimensionless distance run by the slide since the initial time. Notice that continuity conditions of the Duhamel theorem require that $h_s \in C^3$, namely that h_s be continuous together with all derivatives up to the third order. In case of a slide moving with constant speed, and consequently with constant Froude number in a constant-depth ocean, the argument of h_s simplifies to $\sigma = x - \mathrm{Fr}\ t$, and the solution (29) may be written as:

$$\xi(x,t) = \frac{1}{2}\int_{x-t}^{x+t} \partial_q h_s(\chi - \mathrm{Fr}\ q)\big|_{q=0}\,\mathrm{d}\chi + \frac{1}{2}\int_0^t \mathrm{d}q \int_{x-(t-q)}^{x+(t-q)} \mathrm{d}\chi\ \partial_{qq} h_s(\chi - \mathrm{Fr}\ q). \tag{30.2}$$

The integrals in expression (30.2) may be calculated easily and lead to the water elevation:

$$\xi(x,t) = \xi_{\mathrm{F}}(x,t) + \xi_+(x,t) + \xi_-(x,t), \tag{31.1}$$

where

$$\xi_{\mathrm{F}}(x,t) = \frac{\mathrm{Fr}^2}{\mathrm{Fr}^2 - 1} h_s(x - \mathrm{Fr}\ t) \quad \mathrm{Fr} \neq 1, \tag{31.2}$$

$$\xi_+(x,t) = -\frac{1}{2}\frac{\mathrm{Fr}}{\mathrm{Fr} - 1} h_s(x - t) \quad \mathrm{Fr} \neq 1, \tag{31.3}$$

$$\xi_-(x,t) = -\frac{1}{2}\frac{\mathrm{Fr}}{\mathrm{Fr} + 1} h_s(x + t) \quad \mathrm{Fr} \neq 1. \tag{31.4}$$

The water elevation functions (31.2)–(31.4) are in order: 1) the forced wave travelling together with the slide at the same velocity Fr, 2) a free wave propagating toward positive x, and 3) a free wave moving in the opposite direction. What is remarkable in this solution is that the excited tsunami is composed of three distinct waves that are initially superimposed to match the initial conditions, and that separate progressively as time elapses. These waves have the same shape as the landslide body, but with different amplitude and polarity, due to their different dependence on the Fr number. For example, ξ_- is a trough irrespective of the value of Fr, whereas ξ_+ is a trough for Froude numbers larger than 1 and a crest for Froude numbers smaller than 1. Furthermore, the forced wave ξ_{F} always has sign opposite to ξ_+. An alternative derivation of this solution based on the theory of characteristics may be found in the paper by TINTI and BORTOLUCCI (2000a), where the solution for the associated velocities also is provided, together with the solution in the special case of critical

regime (Fr = 1), for which expressions (31) do not hold. In general, for arbitrary time histories of the sliding body, viz. with Froude number depending on time, water elevation in expression (29) cannot be calculated analytically, but must be evaluated numerically, which implies a numerical computation also of the time integral of expression (23.2) to determine the velocity field. Practically, these integrals may be evaluated accurately, but computation time increases along with time coordinate t, and with the time difference $t - q$ between the observation time and the source time, governing the amplitude of the integration intervals of eq. (29). For slides with variable velocities, resulting water waves do not possess the simple form of eqs. (31), but albeit a clear distinction between forced wave and free waves might be more problematic, waves given by (31) constitute a reference solution whereby more general cases may be interpreted usefully and meaningfully, as will be seen in due time.

Linear Tsunami Generation by Landslides in a Sea with Variable Depth

If the sea bottom $h(x)$ has an arbitrary profile depending on x, wave evolution is governed by the set of equations (20) that in nondimensional form may be written as:

$$\xi_t + (uh)_x = \partial_t h_s, \tag{32.1}$$

$$u_t + \xi_x = 0, \tag{32.2}$$

$$u(x,0) = \xi(x,0) = 0. \tag{32.3}$$

It can be reduced then to the second-order differential hyperbolic equation:

$$\xi_{tt} - (h\xi_x)_x = \partial_{tt} h_s, \tag{33.1}$$

$$\xi(x,0) = 0, \tag{33.2}$$

$$\xi_t(x,0) = \partial_t h_s(x,0), \tag{33.3}$$

that is an extension of the corresponding eq. (23.1) that is valid for basins with constant depth. In general, the solution to this problem cannot be found in an explicit form, such as expressions (26) or (28), however there is one remarkable exception that is relevant because it is unique and that we will explore extensively in this paper. Let us assume that the ocean depth is defined by the following dimensional law:

$$h(x) = \left[\frac{h_1^{3/4}(x_2 - x) + h_2^{3/4}(x - x_1)}{x_2 - x_1}\right]^{4/3}. \tag{34.1}$$

There is no loss of generality in presuming $x_2 > x_1$ and $h_2 \geq h_1$. This law specifies that water depth increases together with x according to a power that is not much greater

than unity, which means that the bottom profile has a slope that increases mildly with x and that may be considered constant over distances that are not too large (see Fig. 2a). The above expression transforms to the non-dimensional one-parameter counterpart law:

$$h(x) = (ax + 1)^{4/3} \quad -a^{-1} < x < \infty \tag{34.2}$$

entailing that $h(0) = 1$, and that $h(1) = (a + 1)^{4/3}$, which means that the parameter may be determined as $a = h(1)^{3/4} - 1$ by specifying for instance the water depth at the scaled unit distance from the origin $x = 1$. If we further define a new water elevation η by means of:

$$\eta(x, t) = c(x)^{1/2} \xi(x, t), \tag{35.1}$$

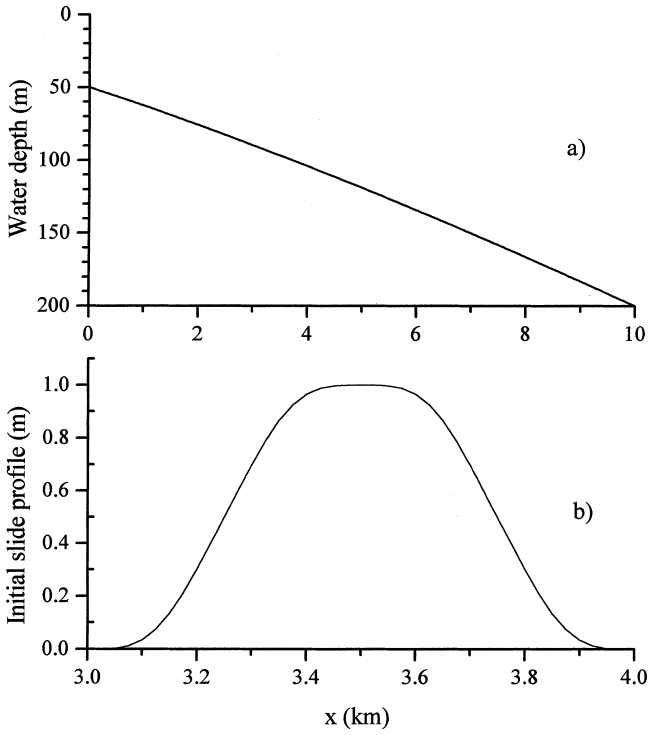

Figure 2

a) Sea-bottom profile $h(x)$ used in the computations. It satisfies the law (34.1) with $h_1 = 50$, $h_2 = 200$, $x_1 = 0$ and $x_2 = 10$ km. Slope is almost constant over the considered interval of the x axis, with slightly downward curvature. b) Initial profile of the slide. It is a 1 km long body, initially placed between 3 and 4 km, and symmetric with respect to its central axis ($x = 3.5$ km). The profile is a curve following the expression given in the Appendix, going very smoothly to zero, to fulfill the continuity conditions required by the Duhamel theorem. Maximum slide height is 1 m, which makes the aspect ratio δ very small and fully respects the condition for linear waves.

$$c(x) = h(x)^{1/2}, \tag{35.2}$$

where, consistent with prior section, $c(x)$ is the nondimensional local water wave celerity, the differential equation (33.1) becomes in terms of the new unknown:

$$\eta_{tt} - c(c\eta_x)_x = c^{1/2}\partial_{tt}h_s. \tag{36}$$

Finally, let us introduce a new independent variable r according to the definition:

$$r(x) = \int_0^x c(\chi)^{-1}\,\mathrm{d}\chi = \frac{3}{a}\left[(ax+1)^{1/3} - 1\right] \quad -a^{-1} < x < \infty \tag{37.1}$$

which implies the associated inverse transformation:

$$x(r) = \frac{1}{a}\left[\left(\frac{a}{3}r + 1\right)^3 - 1\right] \quad -3a^{-1} < r < \infty. \tag{37.2}$$

Notice that, if $c(x)$ is viewed as the local celerity function, coherently it follows that $r(x)$ may be interpreted as the nondimensional time taken by a free wave to travel the distance x from the origin, though formally it plays the role of a space variable. It is now easy to deduce that the unknown η, seen as a function of r and t, viz. $\eta(r,t)$, satisfies the differential problem:

$$\eta_{tt} - \eta_{rr} = c^{1/2}(x(r))\partial_{tt}h_s(x(r),t), \tag{38.1}$$

$$\eta(r,0) = 0, \tag{38.2}$$

$$\eta_t(r,0) = c^{1/2}(x(r))\partial_t h_s(x(r),0), \tag{38.3}$$

that in space (r,t) has the same form as problem (23) in the ordinary space (x,t), and may be solved as well by applying the Duhamel theorem. Hence, the explicit solving expression for $\eta(r,t)$ is:

$$\eta(r,t) = \frac{1}{2}\int_{r-t}^{r+t} c(x(r'))^{1/2}\partial_t h_s(x(r'),0)\,\mathrm{d}r' + \frac{1}{2}\int_0^t \mathrm{d}q \int_{r-(t-q)}^{r+(t-q)} \mathrm{d}r'\; c(x(r'))^{1/2}\partial_{tt}h_s(x(r'),q) \tag{39.1}$$

by means of which it is simple to obtain water elevation, on making use of (37.1) and on inverting (35.1), that is:

$$\xi(x,t) = c(x)^{-1/2}\eta(r(x),t). \tag{39.2}$$

Observe that in space (r,t) both forcing functions, the one in the second-order differential equation (38.1) as well as the one in the initial condition (38.3), are affected by the static factor $c^{1/2}(r)$ that increases with r and is independent from time. In general this factor prevents any simplifications of the formula (39.1) of the type

used for non-deformable landslides that yielded the simple three-wave solution given in eqs. (31). Consequently, the final solution (39) is to be computed by means of the numerical evaluation of the involved integrals.

Computation of Tsunami and Discussion

The theory elucidated in previous sections is applied here to explore the main characteristics of the waves engendered by a submarine body advancing with a prescribed motion along the sea bottom. In the following, use of dimensional quantities will be more convenient to discuss the results. Ocean depth passes from 50 m up to 200 m within the interval of interest here, viz. $x \in [0, 10\ \text{km}]$, according to the law (34.1). Its slope increases slightly with the position x, but may be considered approximately constant, as may be appreciated from plot of Figure 2a. The slide is released from its initial position that is comprised between $x_i = 3$ km and $x_f = 4$ km, has a constant horizontal length $L_S = 1$ km, and for the sake of simplicity it has supposedly a symmetric profile as depicted in Figure 2b. This is a continuous function of its argument $\sigma = x - \mathrm{V}t$ up to the third order of differentiation, to match the requirement of the Duhamel theorem (see Appendix B for further details). The body moves at constant horizontal speed V. Figures 3–5 show the results of experiments carried out for bodies moving at different speeds. In graphs of Figure 3 the body moves at V = 15 m/s, corresponding to a subcritical forcing, namely with Froude number, Fr, smaller than unity (see last panel of Fig. 6). Remembering that Fr is defined as the ratio V/c with $c = (gh(x))^{1/2}$, increasing as depth increases, a subcritical regime entails that the slide is slower than free waves travelling at the speed c. Figure 3 depicts wave elevation profiles at different times. It shows that three waves gradually form as the effect of body motion: one negative wave travelling backward, and a system of two advancing waves. The former is positive and quicker, while the following is negative and proceeds together with the slide. It is important to emphasize that this wave pattern very much resembles that one produced by a slide in a constant-bottom sea (TINTI and BORTOLUCCI, 2000a), and the above three waves correspond respectively to ξ_-, ξ_+, and ξ_F, given in expressions (31). Therefore, analogously to ξ_+, the leading crest here may be interpreted as the free wave travelling forward. Here it has velocity increasing with depth, and its separation from the following forced wave, going with the slide and analogous to ξ_F, increases with time. This similarity is relevant and indeed is expected from a physical point of view, though it cannot be easily seen from mathematical expressions providing the general integral solution (39). There is however an important difference between flat and non-flat ocean cases. In Figure 3, after separation between the leading crest and the following forced trough has taken place, there appears a depression connecting the two impulses that becomes increasingly longer as separation distance increases. At greater times, its amplitude diminishes gradually, though it does not vanish. This

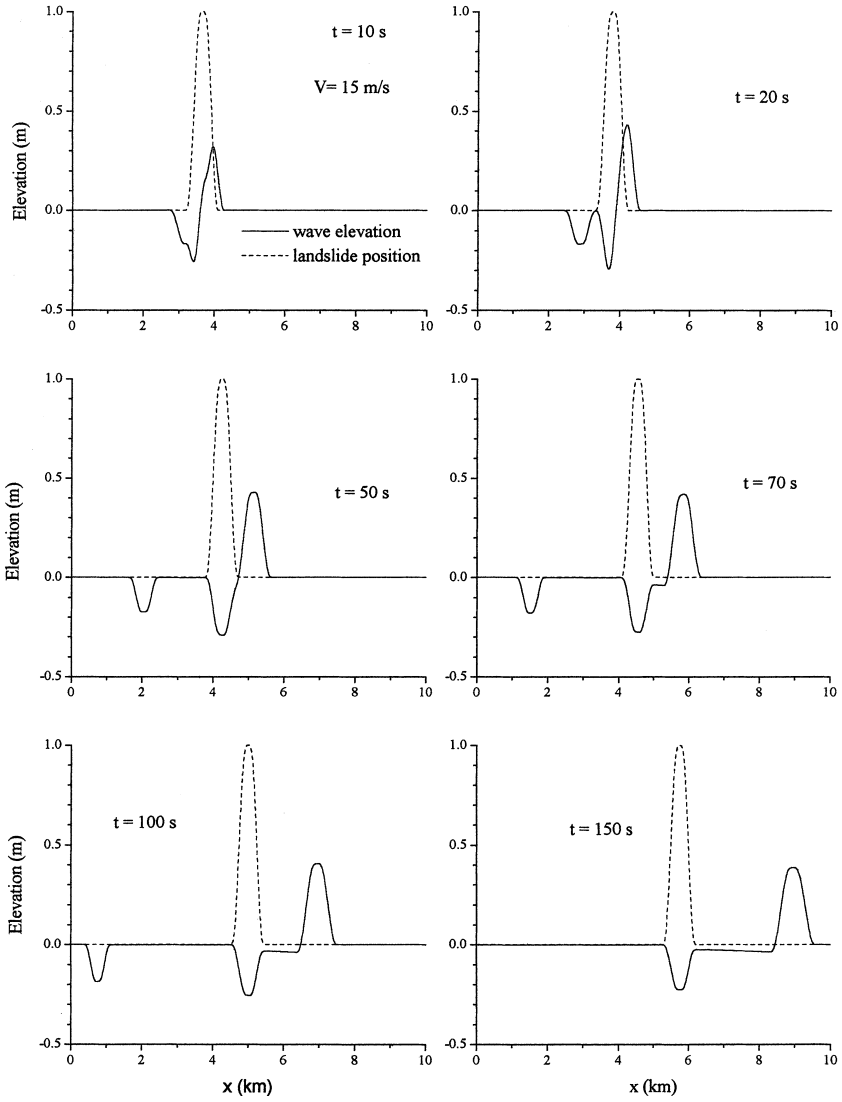

Figure 3
Water wave elevation computed at various times by means of formulas (39). Slide proceeds at subcritical constant horizontal speed. Water surface profile (solid) and slide profile (dashed) are plotted superimposed at the same scale.

connecting depression is absent in waves developed by constant-speed rigid bodies in a flat ocean, and is mostly the effect of Froude number diminishing with time, as will be better seen later. Figures 4 and 5 delineate water elevations produced at various times by bodies moving with respective speeds of 30 m/s and 50 m/s. These speed values are high, however realistic, since similar values have been estimated for

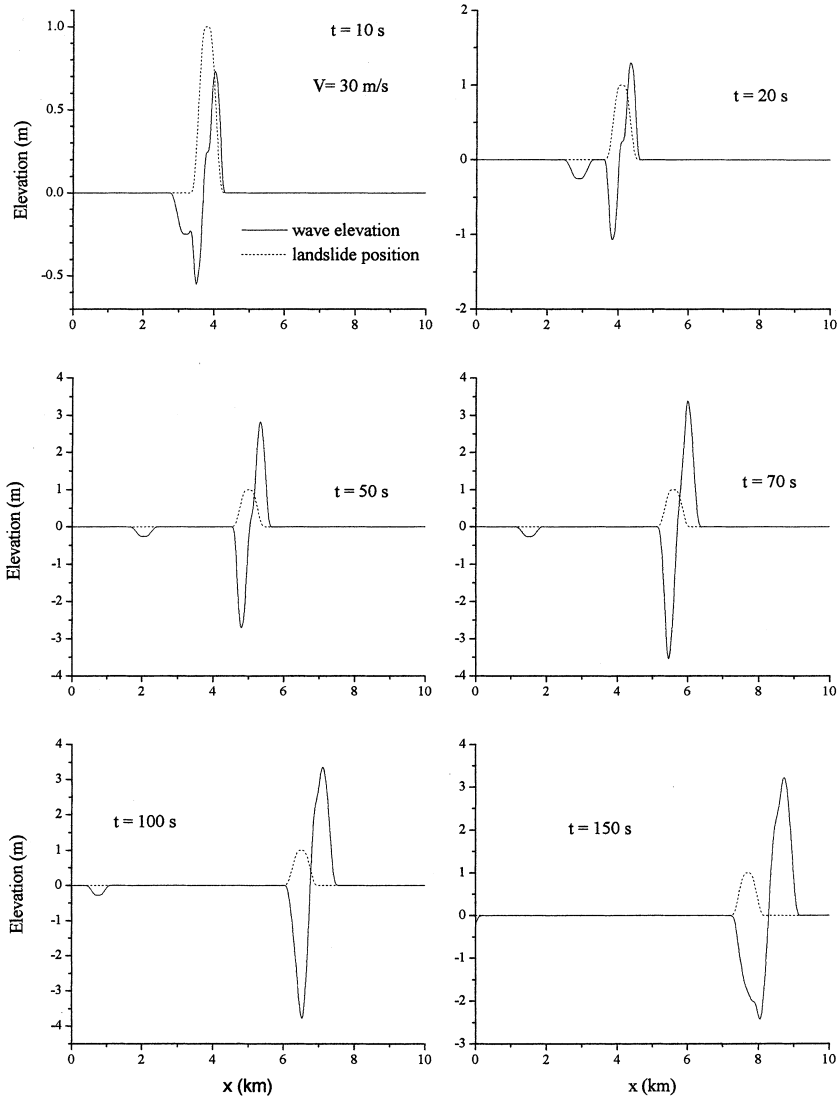

Figure 4
Same as Figure 3. Slide constant velocity of 30 m/s gives rise to subcritical regime, but closer to critical point than the case of Figure 3. Excited waves are larger.

avalanches entering the sea and producing tsunamis (HEINRICH *et al.*, 1999; TINTI *et al.*, 1999b). The former velocity corresponds to a subcritical regime, with Fr closer to critical value than for the first case, whereas the latter coincides with the supercritical condition for the slide, at least within the range of distances used for computations (see also right bottom panels of Figs. 7 and 8, respectively). Wave patterns of Figures 3 and 4 are similar. Since in the second case, the slide is faster and

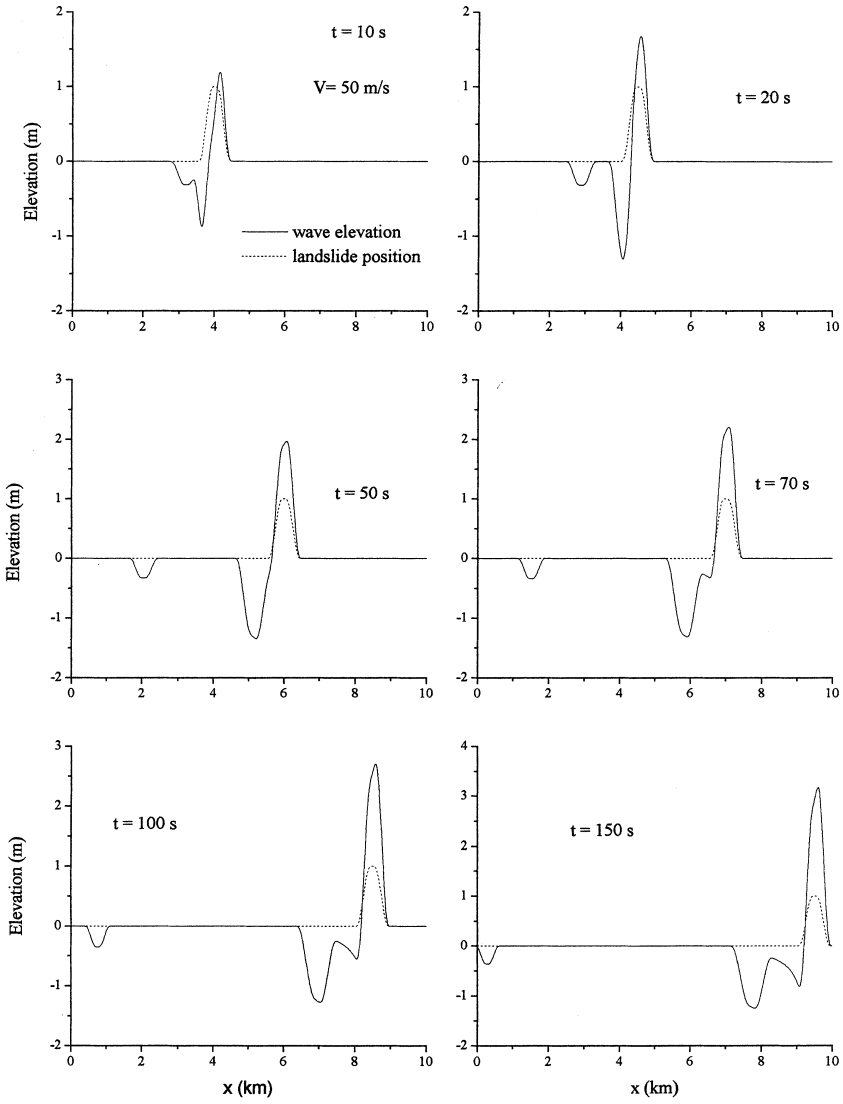

Figure 5
Same as Figure 3. Slide is supercritical and governs progression of the leading crest.

closer to the free wave velocity, separation between the advancing forced and free waves is not yet complete at 150 s, and the intermediate depression is not yet observable at this evolution time. The most relevant difference between the two cases concerns wave amplitude. The slide corresponding to Fr closer to unity excites much larger waves. This is still a feature common to the flat bottom case, as is immediately derivable from formulas (31), where all wave amplification coefficients have

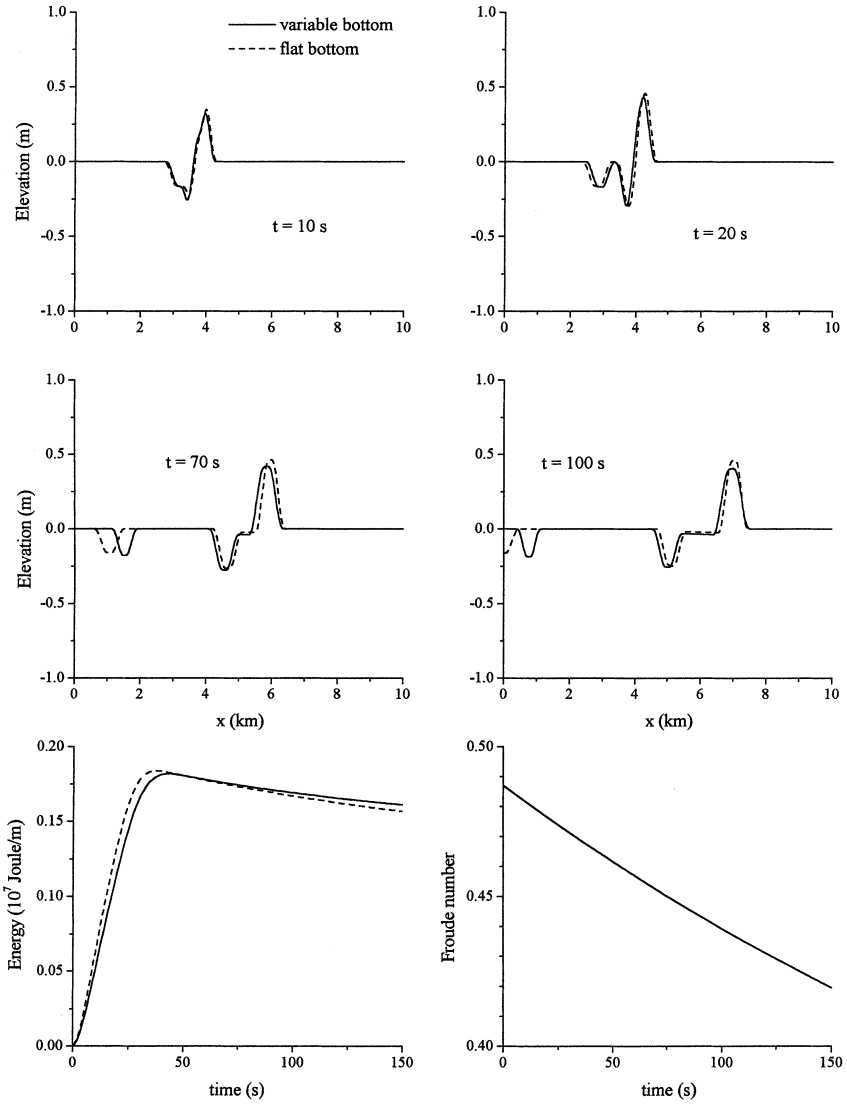

Figure 6
Water wave evolution for variable as well as for equivalent flat bottom ($h = 125$ m). Slide moves underwater with Froude-number time-law shown in the right bottom panel. The left bottom panel displays the energy of the tsunami per unit ocean width. Solid curves are the same as shown in prior Figure 3 and are replicated here to facilitate comparison.

denominators tending to zero as Fr approaches 1. The case of a supercritical slide confirms our previous results, as regards the general wave pattern. It should be noticed that now the leading positive wave may be associated with the forced wave progressing together with the slide, while the free advancing wave is following at a

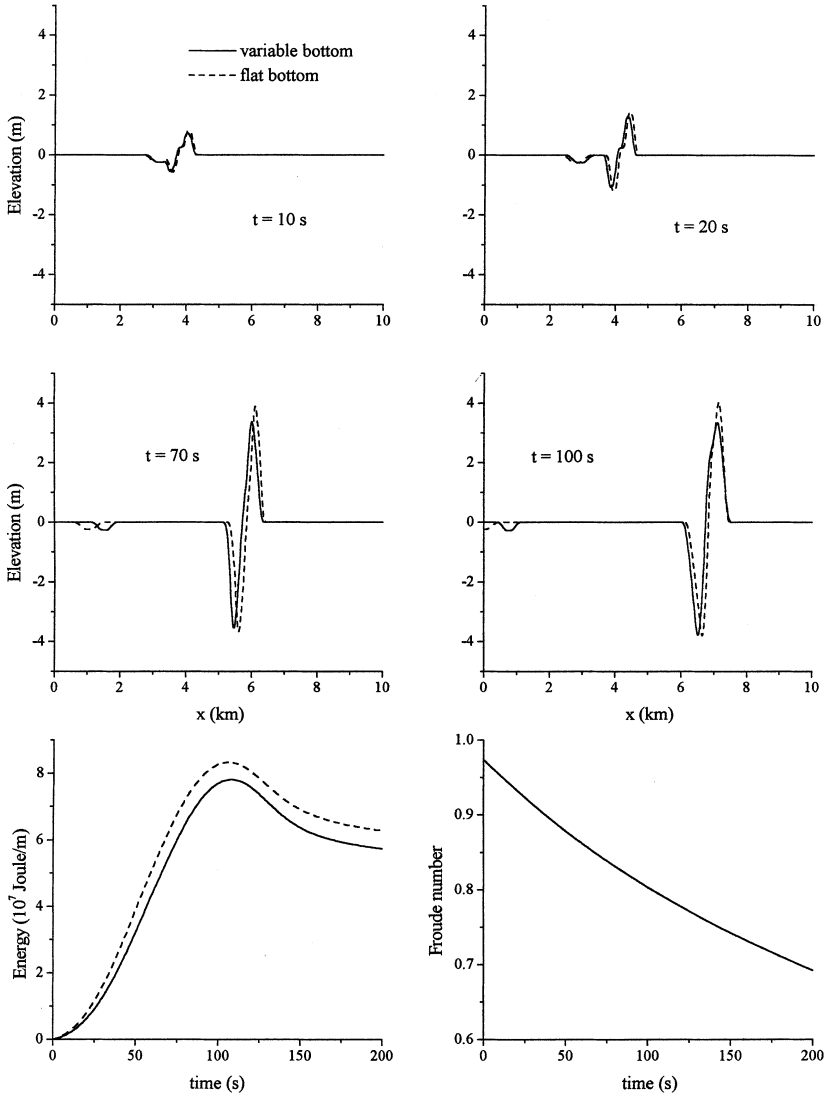

Figure 7
Same as Figure 6. Now Fr time history corresponds to the case exhibited in Figure 4.

distance that increases with time. The connecting depression is large and well visible yet on the 70 s graph.

The strong similarity between linear waves in flat and non-flat seas encourages us to see if the intermediate depression, thus far computed in variable depth, but not in constant depth, may be obtained even in this latter case. For this purpose, we will replicate the three experiments illustrated above in a flat ocean according to the following correspondence rule. A constant-speed slide in variable depth ocean is

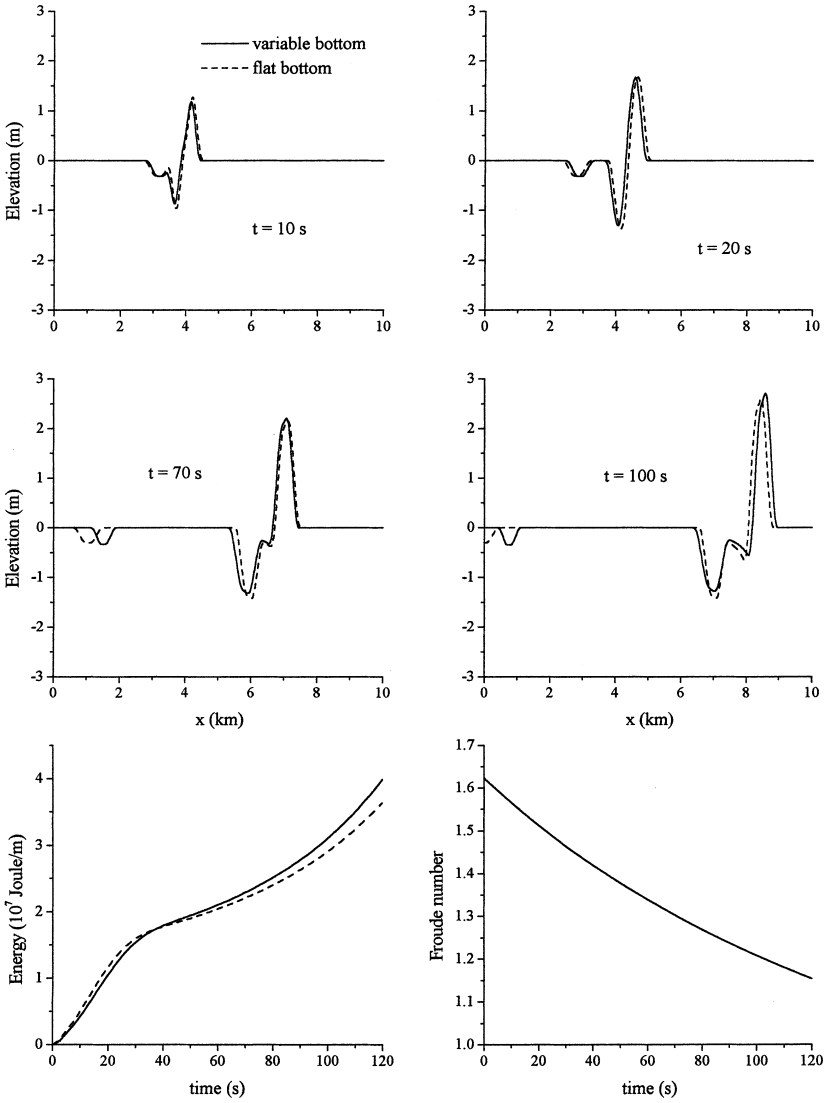

Figure 8
Same as Figure 6. Fr time history is the same as that used for the supercritical slide case treated in Figure 5.

associated with a Froude number that changes with time according to a time history Fr(t) that may be simply computed. We will use the same time history Fr(t) in a flat ocean, which implies consideration of a body moving at variable speed. The solution is calculated by means of the solving formula (29). Notice that one remarkable difference between integral expressions (29) and (39.1), holding for a flat and non-flat bottom respectively, resides in the weighing factor $c(x)^{1/2}$, whose action in (39.1) is

counteracted by the factor $c(x)^{-1/2}$ in the inverse formula (39.2). In the first experiment, Fr is surmised to depend on time according to the law depicted in Figure 6, last panel. It corresponds to the same time history as the slide travelling with a constant speed of 15 m/s in variable depth ocean. An intermediate depth of 125 m has been used for the flat bottom sea. Water elevations in both cases are very similar, though timing is slightly different due to the diverse propagation velocity of free waves in the two oceans. The left bottom panel of Figure 6 shows the energy of the tsunamis which changes with time. Leaving other considerations on energy growth and decrease to the next section, we only outline here that even energy histories are very close one another. Figures 7 and 8 correspond to cases previously illustrated by means of Figures 4 and 5, respectively. Close resemblance between curves calculated for flat and non-flat bottoms under the assumption of equal Froude number time-dependence is strongly confirmed, which demonstrates the essential role of Fr in determining the most important characteristics of the generated waves, such as wave pattern, amplitude, waveform and energy.

Energy of the Tsunami

Energy of the tsunami induced by a bottom disturbance in the shallow-water approximation may be easily shown to satisfy the following dimensional equation in a 1-D ocean with bottom $h(x)$ (TINTI and BORTOLUCCI, 2000a):

$$\psi_t + \rho g \, (h\xi u)_x = \rho g \xi \, \partial_t h_s. \tag{40.1}$$

Here ψ is the density of the total tsunami energy per unit width and unit length of the ocean. The term in the right-hand member of this equation plays the role of an energy source or sink according to its sign being positive or negative. In case of an ocean of constant depth the above expression simplifies to:

$$\psi_t + \rho g h \, (\xi u)_x = \rho g \xi \, \partial_t h_s. \tag{40.2}$$

If we designate the total tsunami energy per unit width as E, i.e., if:

$$E(t) = \int_{-\infty}^{+\infty} \psi(x,t) \, \mathrm{d}x. \tag{41}$$

from (40.2) it descends that:

$$E_t(t) = \rho g \int_{-\infty}^{+\infty} \xi(x,t) \, \partial_t h_s(x,t) \, \mathrm{d}x. \tag{42}$$

The total energy per unit width transferred to the water by the sliding body is at any time obtained by integrating expression (42), that is:

$$E(t) = \int_0^t E_t(\tau)\,\mathrm{d}\tau = \rho g \int_0^t \mathrm{d}\tau \int_{-\infty}^{+\infty} \xi(x,\tau)\partial_\tau h_s(x,\tau)\,\mathrm{d}x. \tag{43}$$

Observe that, though the space integral is extended over the entire x axis, its integrand differs from zero only over a limited interval, since the body has a finite extension. This makes this formula suitable for numerical computations. It has been used to calculate tsunami energy graphs shown in the left bottom panels of Figures 6–8. As far as the product $\xi\,\partial_t h_s$ is positive, energy cumulates in the water, but when it is negative water energy diminishes, and since it is not dissipated within the sea, due to the assumption of inviscid fluid, energy decrease must be associated with energy flow from the water to the body. We will try to better understand the time dependence of tsunami energy by analysing more illustrative examples.

Typically, landslide motion may be considered as characterised by a Froude number time history that is defined over a finite duration interval T_D of hundreds of seconds, with Fr initially increasing rapidly, reaching a peak value and then gradually decreasing and vanishing at time T_D. For example, this is the case of the simulated tsunamigenic flank collapse at Stromboli volcano in the Tyrrhenian Sea, Italy, which presumably occurred in Holocene time and is responsible for the scar known as Sciara del Fuoco (TINTI *et al.*, 1999b). Moreover, generally the regime is subcritical with Froude numbers not exceeding unity even at their peak value, due to the action of water resistance that is effective in slowing down the moving body. Thus there is no loss of generality if we take into account a typical Froude number curve as shown in Figure 9a, that we will designate as Stromboli-like or more simply with code ST in the course of this discussion. In a flat ocean of 100 m depth, the slide first accelerates, reaching a maximum Fr value of about 0.77 at the time $T_M = 44$ s , and then progressively decelerates coming to a stop at the end of the duration interval $T_D = 247$ s. The corresponding energy curve calculated by the aid of eq. (43) is shown in Figure 9b. The energy of the excited water waves increases slowly, attaining the maximum value at about 110 s, and then decreases steadily, but with a diminishing rate until T_D, whereas for later times it remains constant. In order to better understand the characteristics of the initial energy rise, we have considered some other cases illustrated in Figures 9a and 9b, all characterised by the same peak value of Fr. Initially, let us examine the limiting case of a box curve, here named as case Box, with Fr being constant over the entire interval T_D. This simple case, in which the body is virtually subject to infinite acceleration and deceleration at times $t = 0$ s and $t = T_D$ respectively, admits an analytical expression for the water energy $E(t)$ (TINTI and BORTOLUCCI, 2000a). The corresponding energy curve displayed in Figure 9b has a different shape exhibiting a stable plateau, which indicates that the physical system formed by the landslide and the water waves has reached a stationary state, with no further exchange of energy between body and waves. The energy saturation level is attained at the time when the forced wave and the progressing free wave, travelling

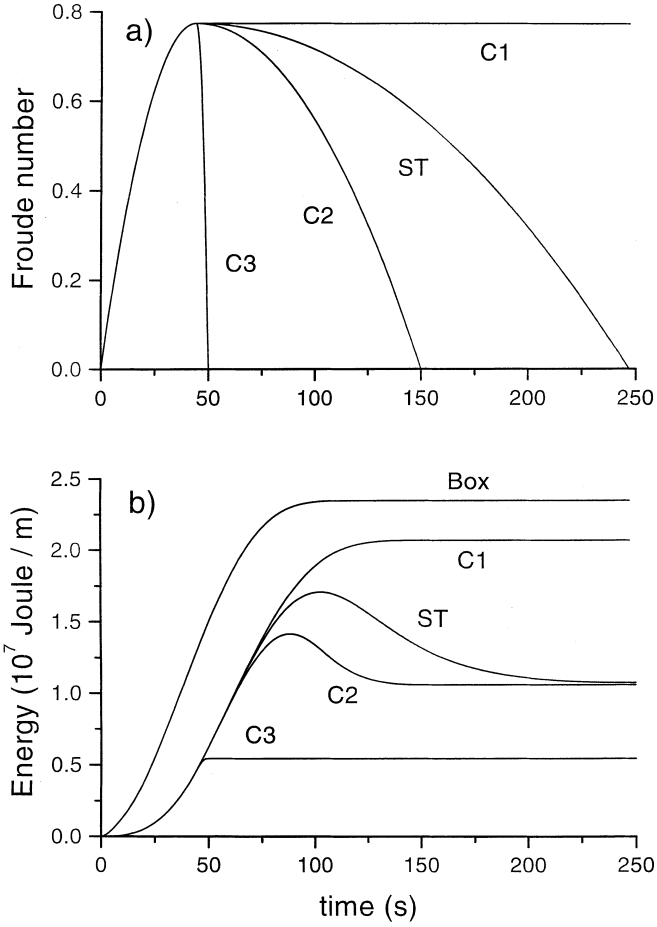

Figure 9
a) Froude number vs. time for cases ST and C1–C3 of subcritical regimes in a flat 100 m deep ocean. Curve denoted by ST is similar to the one associated with the tsunamigenic collapse of the NW flank of Stromboli. b) Corresponding wave energy computed by means of formula (43). Curve coded Box corresponds to a box-like Fr curve, with Fr constant over the interval 0–250 s, not plotted in Figure a), for the sake of readability.

with different velocity, separate from each other. It will be denoted by T_S and called separation time. It is approximately equal to 100 s for our case Box. Additionally it is easy to demonstrate that for box-like excitations a separation time T_S shorter than T_D always implies that the physical system landslide-water has time to reach energy saturation (TINTI and BORTOLUCCI, 2000a). Furthermore, it is worthwhile observing that the curve increases monotonically until the time T_S with a more rapid rise than the case ST. All remaining cases plotted in Figures 9a and 9b and denoted by codes C1–C3 are cases in which the assumed Fr time history is equal to curve ST until T_M,

after which they depart: one remains constant with no Fr decay (C1), whereas the others have faster decreases, and accordingly, shorter duration times (C2 and C3). What can be learned from the associated energy curves portrayed in Figure 9b is that all share the same energy rise, but achieve various energy levels. It is interesting to consider the energy curve of case C1. Energy grows as in case ST and exhibits a well-defined plateau later than 150 s, suggestive of energy saturation, similar to the case-Box curve. However, it attains a smaller energy level because the average Froude number is smaller, and, consequently more distant from critical unitary value. The remaining two cases, characterised by faster Fr drop, correspond to energy curves that do not saturate. Note that for times larger than T_D, energy remains obviously constant because energy rate E_t of expression (42) is identically zero. To summarise, the main findings resulting from all the above experiments can be expressed as follows: given a peak value for Fr, tsunami energy tends to be the larger, 1) the faster is the rise of Fr, or equivalently, the largest is the body acceleration, and 2) the longer is the duration interval T_D, but if saturation condition occurs, increasing T_D produces no further change in tsunami energy level.

To clarify the energy decrease apparent in the energy graphs of Figures 6 and 7 as well as in some of the curves examined above, let us consider further variants, coded C4–C7, of case ST, as proposed in Figure 10a. Here Fr curves are taken to be equal to that of ST until T_M, then to be constant until the time $T_M^* = 150$ s, and then to drop with different rates until T_D, with diverse values of T_D for various cases. Time T_M^* is taken large enough to ensure that saturation takes place, and therefore that the drop of Fr for times later than T_M^* has no influence on the initial growing part of the energy curves. These are plotted in Figure 10b and are perfectly superimposed in the rising phase and in part of the plateau. Subsequently they depart from each other, showing a continuous decrease enduring until the end of the duration interval, after which energy is constant. The energy drop takes longer and is more relevant for Fr number time histories with longer and smoother falls. Notice further that in the limiting case of Fr suddenly dropping to zero (C4), no water energy decrease can take place, and saturation level is maintained. Interestingly, a tsunami with the same saturation energy would be produced by a slide corresponding to a curve with no drop of Fr (case C1): that is, a curve with Fr constant for all times exceeding T_M^*.

Let us consider the case C1, yielding saturation, and compute the corresponding waveforms, and let us then compare them with water elevation profiles computed for one of the non-saturated cases analysed above, such as the ST case. Figure 11 shows snapshots of water waves taken at different times. Expectedly, bearing in mind that Fr curves for the two cases under comparison are identical until $T_M = 44$ s, wave profiles are similar in the first snapshot ($T = 50$ s), but they are also similar until tsunami maximum energy is reached at about 100 s. Next energy curves depart substantially (they are plotted in Figure 9b), and, correspondingly, wavefields are significantly different. The saturation case C1 shows that the advancing wave system is formed by two separated waves, namely the leading free wave and the following

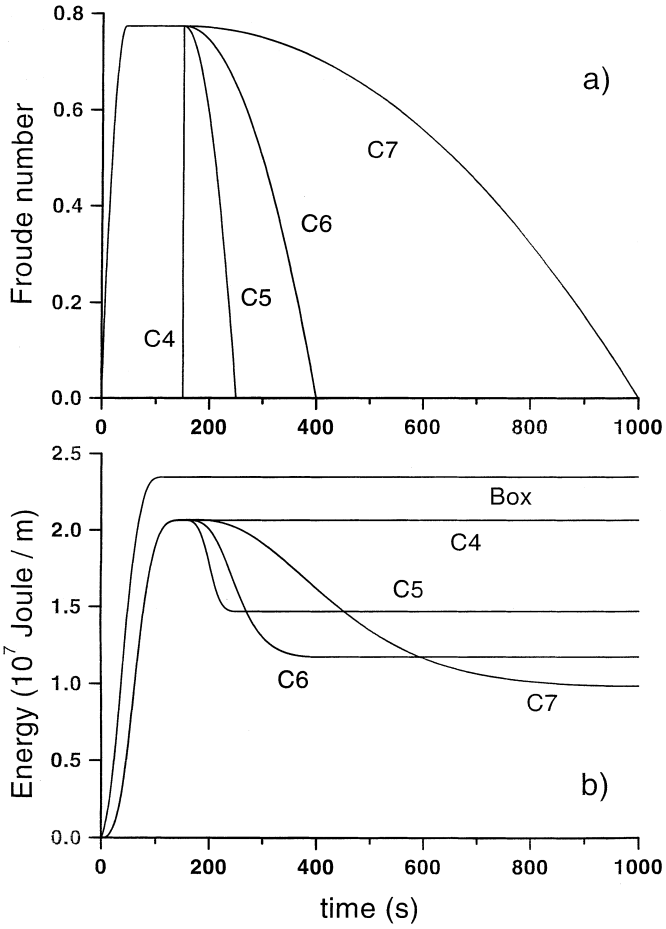

Figure 10
a) Froude number vs. time for cases C4–C7 of subcritical regimes in a flat 100 m deep ocean. b) Corresponding wave energy computed by means of formula (43). Energy curve related to box-like Fr is repeated here from Figure 9b for reference.

forced wave, and that slide and forced wave travelling with the same speed are in nearly perfect opposition, which ensures that energy integral (43) has a net zero value and no energy variation is consequently allowed. Conversely, ST wave profiles illustrate that the leading wave is similar to the leading wave of case C1, but it is followed by a depression connecting it to the slide body and inclined to become longer as time passes. In the slide region the perfect phase opposition between slide and forced wave is lost. The negative wave signal is strongly asymmetrical, and it is precisely its lack of correlation with the slide shape that is responsible for energy subtraction from the water. On the other hand, this trough tends to become increasingly smaller, and therefore energy decrease reduces with time. It is important

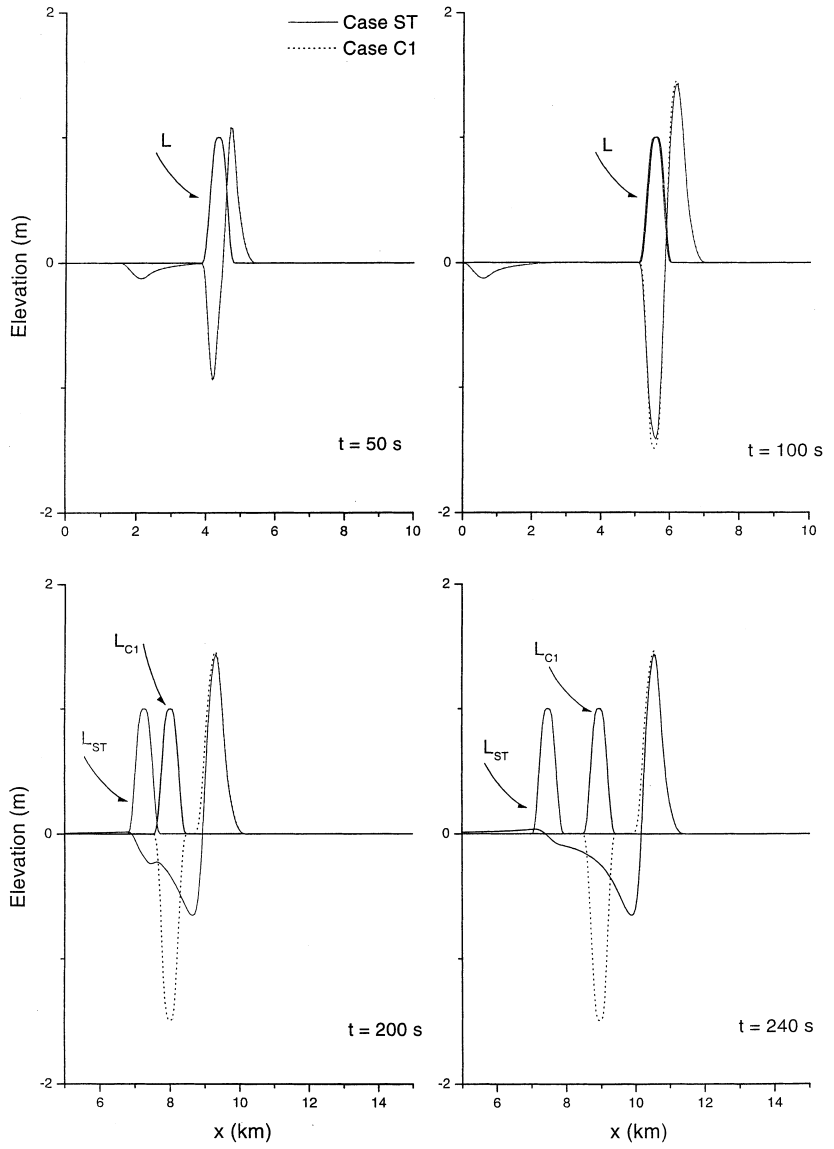

Figure 11
Wave profiles calculated at various times for two different cases: Froude-number time-history of case ST (solid) and a variant of it, case C1, yielding energy saturation (dotted). The two Fr curves are identical until time T_M (44 s), thereafter the latter remains constant. Corresponding positions of the sliding body are also plotted (solid line) and indicated by arrows: after time T_M, the slide of the former case is slower. In the first snapshot ($t = 50$ s) landslides and waves of the two cases are almost perfectly overlapping, which, as regards landslide, is also true for the second snapshot ($t = 100$ s).

to stress that, given the subcritical regime considered in all these examples, these energy variations are mostly associated with the negative trough following the leading wave, and hence the first arriving signal at positions distant from the source region (forward or backward) are not significantly affected by the way in which the Froude number, or equivalently the slide velocity, falls to zero.

Conclusions

A shallow-water approximation has been derived and used to study landslide-generated water waves. Linear theory for flat and non-flat 1-D sea floors has been applied, and analytical expressions for water elevation and water particle velocity in the form of explicit integrals have been found by means of the Duhamel theorem valid for rigid sliding bodies of arbitrary shape and of arbitrary velocity. The case of an ocean depth profile that depends on x according to law (34) has been shown to be amenable to the constant-depth case through a convenient redefinition of unknowns (35) and coordinate transformation (37). Comparison of water waves computed for a flat sea floor as well as for a variable-depth sea has established that slides moving with the same Froude number time histories produce similar waves, as regards wave pattern, wave amplitude and wave energy, which identifies the Froude number as a key parameter to understand wave generation and evolution. Due to this finding, slides on a flat sea floor have been used to study the main characteristics of waves also generated in oceans with variable depth. The system of the produced waves comprises three main pulses: one moves backward (in the opposite direction of slide motion) as a free wave, and two move forward. Of these two, one travels as a free wave, while the other moves together with the slide as a forced wave. The leading front is the forced wave in the supercritical regime and the free wave in subcritical flow. The leading front is always positive and is followed by a trough. In the case of the Froude number changing with time, the advancing pulses are connected by a depression that becomes longer and smaller as time progresses. Total energy of the water waves can be computed by means of formula (43), and forcing by slides moving with different time histories has been used to investigate energy time evolution. Normally, in real events the maximum Fr number is smaller than 1 since water resistance prevents the slide from attaining high velocities, and hence energy analysis has been confined to subcritical regimes. Typical Fr functions are rapidly increasing until a time T_M when they have a maximum, and then decrease slowly, vanishing at time T_D. In the analysis the two phases (Fr rise and Fr drop) can be conveniently distinguished and separated. The ideal case in which forcing occurs through a box-like Fr function can be interpreted as a special curve with $T_M = 0$. A case, called case ST since its Fr curve is close to the one computed for a Holocene tsunamigenic landslide at Stromboli volcano, is used as a typical reference case. Comparing the box-like curve with curve ST, it has been found that box-like forcing

is more effective in transferring energy to the water, suggesting that initial strong Fr rise (corresponding to short T_M and to strong initial acceleration) favours formation of energetic tsunamis. Furthermore, the former gives rise to energy saturation, however the latter does not. By energy saturation it is meant that tsunami energy reaches its maximum possible value, which depends on Fr, and that further forcing cannot result in a further increase of wave amplitude. Energy saturation occurs if box-like forcing endures for a sufficiently long time (duration interval T_D longer than separation interval T_S). Considering Fr functions equal to ST until T_M and then decreasing with different slope (see cases C2 and C3) demonstrates that the total tsunami energy is smaller for cases with smaller duration time. If Fr functions are equal to ST until T_M, then they are constant until T_M^*, after which they fall to zero over different intervals of time (cases C4–C7), consequently two interesting results are obtained. It is found that all energy curves saturate, provided that T_M^* is sufficiently large, and it also is found that tsunami energy decrease takes place, which is slower, but larger, for slower Fr falls. Analysis of waveforms has revealed that water energy diminution is related to the water depression connecting the leading wave with the following trough, which is typical of variable Froude number curves, and that it mostly involves the trough associated with the slide motion. On the contrary, the leading wave as well as the backward propagating wave are practically unaffected by this process, tending to preserve their own energy. This observation is important since it regards first tsunami arrivals that are generally the most dangerous waves and reveals that their waveform and energy, and, accordingly, their damaging potential, are mostly determined by the first phases of body motion (Fr rise) rather than by its later dynamics.

In conclusion, it is worthwhile stressing the main hypotheses that are the basis of the shallow-water approximation derived in this paper. These are related to the scaling parameters given in equations (8)–(10) of the main text as well as in the corresponding equations (A2) and (A4) of the Appendix A. Essentially, the present theory is appropriate for problems where a unique horizontal scale k and a unique time scale (T or t_c) can be considered for the moving body and for the excited water waves. In all the examples, the body length L_S and the wavelength have the same order of magnitude, as well the body velocity V and the free wave celerity c. An analogous assumption is made for the amplitude of the wave and of the height of the body: their respective scales d and d_s are thought to be equal (see e.g., the position (A4.1)). On the other hand, different scales are taken for the horizontal component U and the vertical component W of the fluid-particle velocity, and for the horizontal length k and vertical length D of the motion, with $\varepsilon = D/k = W/U \ll 1$. The nonlinear shallow-water theory is a consequence of the above set of assumptions and can be further simplified to a set of linear equations if the ratio $\delta = d/D$ is postulated to be at least of order ε. Notwithstanding the restrictions listed here, the theory we have worked out can be used to explore water wave generation by underwater moving bodies in practical cases. The nonlinear approach is appropriate when the

size of the moving body is very large, with a horizontal dimension considerably larger than the local water depth, whereas the linear approach requires the further limitation that the slide thickness be substantially smaller than the local water depth. For example, failures of slopes involving huge sediment bodies with lengths and widths of several kilometres and thickness of several meters or tens of meters, are rare but not exceptional events in ocean depths of 1–2 km relative to the continental shelf margins (HARBITZ, 1992; HAMPTON *et al.*, 1996). Furthermore, the theory can also be applied to smaller mass failures in shallower coastal waters, where the water depth is about several tens or some hundreds of meters, and the requirement of the theory on the body size results in being modified accordingly: about 1 km in width and in length, and about 10 m in height.

Finally, it is worth mentioning that the investigation presented in this paper has been continued in another paper (TINTI and BORTOLUCCI, 2000b), where the solving equation (29) has been further elaborated to place in evidence the dependence of the wave elevation ξ on the acceleration of the moving body. Furthermore, Froude time histories that are typical of bodies sliding along constant slopes have been considered (see WATTS, 1998), and it has been shown that useful estimates of the amplitude of the leading waves propagating forward (in the direction of the body) and backward can be based on the average values of the Froude number taken over suitable initial time intervals.

Appendix A

The system of equations (1)–(7) can be made dimensionless by introducing the appropriate scale for all variables. Let us introduce the scales k, D and T, respectively for the horizontal coordinates x, y, for the vertical coordinate z and for the time t. Let us further introduce the scales U and W for the horizontal components of the fluid particle velocity u, v and for the vertical component w. The pressure scale of the ratio p/ρ is denoted by P. Finally, the scales for the water wave elevation ξ, the ocean depth h and the slide height h_s are designated by d, H and d_s, respectively. Dimensionless variables may be defined to be the ratio of the corresponding variable to the proper scale. For example, the nondimensional ocean depth h' is given by h/H. Upon substituting the dimensionless variables in the equations (1)–(7), it is then easy to derive the corresponding version of the equations:

$$\frac{U}{k}\,(u_x + v_y) + \frac{W}{D}\,w_z = 0, \tag{A1.1}$$

$$\frac{U}{T}\,u_t + \frac{U^2}{k}\,(uu_x + vu_y) + \frac{WU}{D}\,wu_z + \frac{P}{k}\,p_x = 0, \tag{A1.2}$$

$$\frac{U}{T}\,v_t + \frac{U^2}{k}\,(uv_x + vv_y) + \frac{WU}{D}\,wv_z + \frac{P}{k}\,p_y = 0, \tag{A1.3}$$

$$\frac{W}{T}\, w_t + \frac{UW}{k}\,(uw_x + vw_y) + \frac{W^2}{D}\, ww_z + \frac{P}{D}\, p_z + g = 0, \tag{A1.4}$$

$$\frac{W}{k}\, w_y = \frac{U}{D}\, v_z \quad \frac{U}{D}\, u_z = \frac{W}{k}\, w_x \quad \frac{U}{k}\, u_y = \frac{U}{k}\, v_x, \tag{A1.5}$$

$$\frac{d}{T}\, \xi_t + \frac{Ud}{k}\,(u\xi_x + v\xi_y) = Ww \quad \text{at } Dz = \mathrm{d}\xi, \tag{A1.6}$$

$$Pp = 0 \quad \text{at} \quad Dz = \mathrm{d}\xi, \tag{A1.7}$$

$$\frac{UH}{T}\,(uh_x + vh_y) + Ww = \frac{d_s}{T}\, \partial_t h_s \quad \text{at} \quad Dz = -Hh + d_s h_s \tag{A1.8}$$

where the prime denoting dimensionless variables has been dropped for convenience. The nine scale factors that are associated with the above problem are lengths (d, d_s, H, k, D), velocities (U, W), pressure per unit density (P) and time (T), whose dimensions involve only 2 independent reference quantities: length and time, or alternatively, length and velocity. In virtue of the Buckingham's Pi theorem (see FOX and MCDONALD, 1985), it is then possible to introduce $9 - 2 = 7$ independent dimensionless parameters Π_i $(i = 1, 2, \ldots, 7)$, that can be used to describe completely the physical problem. Here, it is convenient to consider the reference length k and the reference velocity $c = P^{1/2}$, whereby it is possible to define the following set of dimensionless parameters:

$$\Pi_1 = d/k, \tag{A2.1}$$

$$\Pi_2 = d_s/k, \tag{A2.2}$$

$$\Pi_3 = H/k, \tag{A2.3}$$

$$\Pi_4 = D/k, \tag{A2.4}$$

$$\Pi_5 = U/c, \tag{A2.5}$$

$$\Pi_6 = W/c, \tag{A2.6}$$

$$\Pi_7 = Tc/k. \tag{A2.7}$$

It is then straightforward to rewrite the equations (A1) in terms of the parameters Π_i:

$$\frac{\Pi_4\Pi_5}{\Pi_6}(u_x + v_y) + w_z = 0, \tag{A3.1}$$

$$\frac{\Pi_5}{\Pi_7} u_t + \Pi_5^2\,(uu_x + vu_y) + \frac{\Pi_5\Pi_6}{\Pi_4}\, wu_z + p_x = 0, \tag{A3.2}$$

$$\frac{\Pi_5}{\Pi_7} v_t + \Pi_5^2\,(uv_x + vv_y) + \frac{\Pi_5\Pi_6}{\Pi_4}\, wv_z + p_y = 0, \tag{A3.3}$$

$$\frac{\Pi_4\Pi_6}{\Pi_7}\, w_t + \Pi_4\Pi_5\Pi_6\,(uw_x + vw_y) + \Pi_6^2\, ww_z + p_z + 1 = 0, \tag{A3.4}$$

$$\frac{\Pi_4\Pi_6}{\Pi_5}\, w_y = v_z \quad u_z = \frac{\Pi_4\Pi_6}{\Pi_5}\, w_x \quad u_y = v_x, \tag{A3.5}$$

$$\frac{\Pi_1}{\Pi_6\Pi_7}\, \xi_t + \frac{\Pi_1\Pi_5}{\Pi_6}\, (u\xi_x + v\xi_y) = w \quad \text{at} \quad z = \frac{\Pi_1}{\Pi_4}\, \xi, \tag{A3.6}$$

$$p = 0 \quad \text{at} \quad z = \frac{\Pi_1}{\Pi_4}\, \xi, \tag{A3.7}$$

$$\frac{\Pi_4\Pi_5}{\Pi_6}\, (uh_x + vh_y) + w = \frac{\Pi_2}{\Pi_6\Pi_7}\, \partial_t h_s \quad \text{at} \quad z = -\frac{\Pi_3}{\Pi_4} h + \frac{\Pi_2}{\Pi_4} h_s. \tag{A3.8}$$

The system of equations (A3) is perfectly equivalent to the set of equations (1)–(7) as well as to the system of equations (A1). No physical hypothesis has been made to date on the values of the scales and of the parameters Π_i. The use of the Buckinghams Pi theorem serves to elucidate that the full problem depends upon seven parameters that can be chosen freely. In general different choices of the parameters lead to different solutions and are useful to describe different classes of phenomena and waves. In this paper the main focus centers on the generation of shallow-water waves by underwater landslides. With this objective in mind, the set of equations (A3) can be simplified by making proper assumptions on the parameters Π_i. In fact, after introducing the following hypotheses:

$$\Pi_1 = \Pi_2 = \Pi_5 = \delta, \tag{A4.1}$$

$$\Pi_3 = \Pi_4 = \varepsilon, \tag{A4.2}$$

$$\Pi_6 = \varepsilon\delta, \tag{A4.3}$$

$$\Pi_7 = 1, \tag{A4.4}$$

where δ and ε are two parameters defined by equations (8) in the main text, the space of the parameters Π_i is reduced from 7 to 2 independent dimensions, and can be handled in an easier way. By making use of the positions (A4), the set of equations (A3) can be transformed into the equations (11.1)–(11.8), from which the nonlinear shallow-water approximation can be deduced through the series-expansion method explained in the text under the assumption that ε is much smaller than unity. Postulating further that $\delta = \varepsilon$ leads to the linear shallow-water approximation that is thoroughly discussed in this paper.

We remark that the features of the solutions depend both on the set of options (A4), that form a set of *a priori* established constraints, and on the resulting governing equations that impose dynamical constraints. To this latter category belongs the property that the water pressure is hydrostatic. Indeed equation (11.4), that entails equation (13.4) in the zeroth-order expansion, implies that the scale P is equal to gD. As a consequence, the reference velocity c has the value $(gD)^{1/2}$ (see eq. (9)), which is the travelling velocity of the free shallow-water waves. On the other hand, some important characteristics of the solution belong to the former class. For

example, assuming $\Pi_1 = \Pi_2$ has the meaning that we seek for solutions in which the water waves excited by the moving body have amplitude with the same order of magnitude as the landslide thickness. Moreover, the ratio $\Pi_6/\Pi_5 = \varepsilon$ means that the vertical velocity is considerably smaller than the horizontal velocity of the fluid particles. It is most interesting to observe that postulating that Π_7 equals 1 entails that the relevant time scale considered in the study is that of the free waves rather than that of the landslide motion. This could sound unreasonable since the cause of the waves is the motion of the landslide itself, and the landslide velocity $\mathrm{V}(t)$ is expected to be a key-quantity of the water generation process. Indeed, both velocities c and $\mathrm{V}(t)$ influence the features of the excited water waves, and correspondingly two time scales could be identified for the process. In this paper we are particularly interested in the waves that are excited when these velocities, though distinct, have the same order of magnitude, making possible the adoption of a unique time scale. Indeed, we will study the waves produced when the ratio $\mathrm{V}(t)/c$, that is called Froude number in the text, is of order unity, discussing wave features in the cases of subcritical ($\mathrm{V}(t) < c$), critical ($\mathrm{V}(t) = c$) and supercritical ($\mathrm{V}(t) > c$) regimes.

Appendix B

The slide profile used in computing all solutions presented in this paper is a function $h_s(\sigma)$ of argument σ and is continuous up to the third order of differentiation with respect to σ. The slide moves with constant horizontal speed V, has length L_S, and its initial position is comprised between the extremes x_i and $x_f = x_i + L_S$. Its mathematical expression is given by:

$$\sigma = x - \mathrm{V}t, \tag{B1}$$

$$h_s(\sigma) = 0 \quad \sigma \in [x_i, x_f], \tag{B2}$$

$$h_s(\sigma) = \frac{A}{4\pi^2}\left\{\frac{1}{2}\Phi(\sigma, x_i)^2 + \cos[\Phi(\sigma, x_i)] - 1\right\}, \quad \sigma \in [x_i, x_i + L_S/4], \tag{B3}$$

$$h_s(\sigma) = \frac{A}{4\pi^2}\left\{-\frac{1}{2}\Phi(\sigma, x_i)^2 + \cos[\Phi(\sigma, x_i)] + 4\pi\Phi(\sigma, x_i) + 1 + 4\pi^2\right\},$$
$$\sigma \in [x_i + L_S/4, x_i + 3L_S/4], \tag{B4}$$

$$h_s(\sigma) = \frac{A}{4\pi^2}\left\{\frac{1}{2}\Phi(\sigma, x_i)^2 + \cos[\Phi(\sigma, x_i)] - 8\pi\Phi(\sigma, x_i) - 1 + 32\pi^2\right\},$$
$$\sigma \in [x_i + 3L_S/4, x_f], \tag{B5}$$

where

$$\Phi(\sigma, x_i) = \frac{8\pi}{L_S}(\sigma - x_i), \tag{B6}$$

and A is the maximum height of the slide. In the experiments carried out in the paper, the slide is supposed to have the amplitude of 1 m and the length of 1 km. Since in linear theory the amplitude of the excited waves is proportional to the body height (see e.g., the solving expressions (29) and (39)), the above choice of unitary slide height is not restrictive. The results shown in the paper can be straightforwardly applied to a body of arbitrary thickness, provided however that the limitations required by the linear shallow-water approximation are respected ($D/k \ll 1, d_s/D \ll 1$).

Acknowledgements

This work was financed by the Italian Ministry of University and Scientific and Technological Research (MURST), and by a contract of the European Communities (INTAS-RFBR-95-1000).

References

Aida, I. (1969), *Numerical Experiments for the Tsunami Propagation – The 1964 Niigata Tsunami and the 1968 Tokachi-oki Tsunami*, Bull. Earthq. Res. Inst. *47*, 673–700.

Assier Rzadkiewicz, S., Mariotti, C., and Heinrich, Ph. (1997), *Numerical Simulation of Submarine Landslides and their Hydraulic Effects*, J. Waterway, Port, Coastal, and Ocean Eng., ASCE *123*, 149–157.

Calvari, S., and Thanner, L. H. (1999), *Etna Avalanche Deposit Prompts Call for Hazard Reassessment*, EOS Trans. AGU *80*, pp. 345, 347–348.

Chubarov, L. B., Shokin, Y. I., and Gusiakov, V. K. (1984), *Numerical Simulation of the 1973 Shikotan (Nemuro-oki) Tsunami*, Computer and Fluids *12*, 123–132.

Davies, H. L. (1999), *Tsunami PNG 1998*, National Library of Papua New Guinea, 48 pp.

Fine, I. V., Rabinovich, A. B., Kulikov, E., Thomson, R. E., and Bornhold, B. D. (1999), *Numerical Modelling of Landslide-generated Tsunamis with Application to the Skagway Harbor Tsunami of November 3, 1994*, International Conference on Tsunamis, Paris, France, May 26 to 28, 1998, published by Commissariat à l'Energie Atomique (CEA), 212–223.

Folland, B. G., *Introduction to Partial Differential Equations* (Princeton University Press, 1995) pp. 174–176.

Fox, R. W., and McDonald, A. T., *Introduction to Fluid Mechanics* (John Wiley and Sons, New York, 1985) pp. 295–330.

Friedrichs, K. O. (1948), *On the Derivation of Shallow Water Theory* (Appendix to *The Formation of Breakers and Bores*, by J. J. Stoker), Comm. Pure Applied Math. *1*, 81–85.

Grilli, S., and Watts, P. (1999), *Modeling of Waves Generated by a Moving Submerged Body. Applications to Underwater Landslides*, Engineering Analysis with Boundary Elements *23*, 645–656.

Hammack, J. L. (1973), *A Note on Tsunamis: Their Generation and Propagation in an Ocean of Uniform Depth*, J. Fluid Mech. *60*, 769–799.

Hampton, M. A., Lee, H. J., and Locat, J. (1996), *Submarine Landslides*, Rev. Geophys. *34*, 33–59.

Harbitz, C. B. (1992), *Model Simulation of Tsunamis Generated by Storegga Slides*, Marine Geology *104*, 1–21.

Harbitz, C. B., and Elverhøi, A. (1999), *On tsunami characteristics and submarine dynamics*, International Conference on Tsunamis, Paris, France, May 26 to 28, 1998, published by Commissariat à l'Energie Atomique (CEA), pp. 257–266.

HEINRICH, Ph., GUIBOURG, S., MANGENEY, A., and ROCHE, R. (1999), *Numerical Modeling of a Landslide-generated Tsunami Following a Potential Explosion of the Montserrat Volcano*, Phys. Chem. Earth *24*, 163–168.

ICHIYE, T., *Tsunami generation as finite depth Cauchy-Poisson problem or long wave problem*. In *Tsunamis – Their Science and Engineering* (eds. Iida, K., and Iwasaki, T.) (Terra Scientific Publishing Company (TERRAPUB), Tokyo 1983) pp. 265–274.

IMAMURA, F., and GICA, E. C. (1996), *Numerical Model for Tsunami Generation Due to Subacqueous Landslide along a Coast*, Science of Tsunami Hazards *14*, 13–28.

IWASAKI, S. (1982), *Experimental Study of a Tsunami Generated by a Horizontal Motion of a Sloping Beach*, Bull. Earthq. Res. Inst. *57*, 239–262.

JIANG, L., and LEBLOND, P. H. (1993), *Numerical Modeling of an Underwater Bingham Plastic Mudslide and the Waves which it Generates*, J. Geophys. Res. *98*, 10,303–10,317.

JOHNSGARD, H., and PEDERSEN, G. (1996), *Slide-Generated Waves in Near-shore Regions. A Lagrangian Description*, Phys. Chem. Earth *21*, 45–49.

KAJIURA, K. (1970), *Tsunami Source, Energy and the Directivity of Wave Radiation*, Bull. Earthq. Res. Inst., Univ. Tokyo, *48*, 835–869.

KAWATA, Y., BENSON, B. C., BORRERO, J. C., DAVIES, H. L., DE LANGE, W. P., IMAMURA, F., LETZ, H., NOTT, J., and SYNOLAKIS, C. E. (1999), *Tsunami in Papua New Guinea was as Intense as First Thought*, EOS, Transactions, AGU *80*, pp. 101, 104–105.

MILLER, D. J. (1960), *Giant Waves in Lituya Bay*, U.S. Geol. Surv. Prof. Paper *354-C*, 51–83.

MURTY, T. S. (1977), *Seismic Sea Waves. Tsunamis*, Bull. No. 198 of the Fisheries Research Board of Canada, Ottawa, 1977, 337 pp.

NODA, E. K. (1970), *Water Waves Generated by Landslides*, J. Waterways, Harbors and Coastal Engineering, ASCE *96*, 835–858.

NODA, E. K. (1971), *Water Waves Generated by a Local Surface Disturbance*, J. Geophys. Res. *76*, 7389–7400.

PELINOVSKY, E., and POPLAVSKY, A. (1996), *Simplified Model of Tsunami Generation by Submarine Landslides*, Phys. Chem. Earth *21*, 13–17.

PEREGRINE, D. H., *Equations of water waves and the approximation behind them*. In *Waves on Beaches and Resulting Sediment Transport* (ed. Meyer, R. E.) (Academic Press 1972) pp. 95–121.

PIATANESI, A., and TINTI, S. (1998), *A Revision of the 1693 Eastern Sicily Earthquake and Tsunami*, J. Geophys. Res. *103*, 2749–2758.

RANEY, D. C., and BUTLER, H. L. (1975), *A Numerical Model for Predicting the Effects of Landslide-generated Water Waves*, U.S. Army Eng. Waterw. Exp. Stn., Res. Rep. No H-75-1.

SABATIER, P. C. (1983), *On Water Waves Produced by Ground Motions*, J. Fluid Mech. *126*, 27–58.

SELLS, C. C. L. (1965), *The Effect of a Sudden Change of Shape of the Bottom of a Slightly Compressible Ocean*, Phil. Trans. Roy. Soc. *A258*, 495–528.

SKLARZ, M. A., SPIELVOGEL, L. Q., and LOOMIS, H. G. (1979), *Numerical Simulation of the 29 November 1975 Island of Hawaii Tsunami by the Finite-element Method*, J. Phys. Oceanography *9*, 1022–1031.

STOKER, J. J., *Water Waves*, Pure Appl. Math. *IV* (Interscience Publishers Inc., New York (1957)) 567 pp.

TAKAHASHI, R. (1943), *On Seismic Sea Waves Caused by Deformation of the Sea Bottom*, Bull. Earthq. Res. Inst. *20*, 375–398 (in Japanese).

TAKAHASHI, R. (1948), *On Seismic Sea Waves Caused by Deformation of the Sea Bottom, The Third Report. The One-dimensional Source*, Bull. Earthq. Res. Inst. *25*, 5–9.

TAPPIN, D. R., MATSUMOTO, T., WATTS, P., SATAKE, K., MCMURTRY, G. M., MATSUYAMA, M., LAFOY, Y., TSUJI, Y., KANAMATSU, T., LUS, W., IWABUCHI, Y., YEH, H., MATSUMOTU, Y., NAKAMURA, M., MAHOI, M., HILL, P., CROOK, K., ANTON, L., and WALSH, J. P. (1999), *Sediment Slump Likely Caused 1998 Papua New Guinea Tsunami*, EOS, Transactions, AGU *80*, pp. 329, 334 and 340.

TINTI, S., GAVAGNI, I., and PIATANESI, A. (1994), *A Finite-element Numerical Approach for Modelling Tsunamis*, Annali Geofisica *37*, 1009–1026.

TINTI, S., and PIATANESI, A. (1996), *Numerical Simulations of the Tsunami Induced by the 1627 Earthquake Affecting Gargano, Southern Italy*, J. Geodynamics *21*, 141–160.

TINTI, S., BORTOLUCCI, E., ARMIGLIATO, A. (1999a), *Numerical Simulation of the Landslide-induced Tsunami of 1988 in Vulcano Island, Italy*, Bull. Volcanol. *61*, 121–137.

TINTI, S., ROMAGNOLI, C., and BORTOLUCCI, E. (1999b), *Modeling a Possible Holocenic Landslide-induced Tsunami at Stromboli Volcano, Italy*, Phys. Chem. Earth *24*, 423–429.

TINTI, S., and BORTOLUCCI, E. (2000a), *Energy of Water Waves Induced by Submarine Landslides*, Pure appl. geophys. *157*, 281–318.

TINTI, S., and BORTOLUCCI, E. (2000b), *Analytical Investigation on Tsunamis Generated by Submarine Slides*, Annali di Geofisica *43*, 519–536.

TUCK, E. O., and HWANG, L.-S. (1972), *Long-wave Generation on a Sloping Beach*, J. Fluid Mech. *51*, 449–461.

VILLENEUVE, M., and SAVAGE, S. B. (1993), *Nonlinear, Dispersive, Shallow-water Waves Developed by a Moving Bed*, J. Hydraulic Res. *31*, 249–266.

YAMASHITA, T., TAKABAYASHI, T., and TSUCHIYA, Y., *Numerical simulation of 1993 July 12 tsunami near Hokkaido; its propagation and flooding onto Aonae district, Okushiri island.* In *Perspectives on Tsunami Hazard Reduction* (ed. Hebenstreit, G.) (Kluwer Academic Press, 1997) pp. 83–97.

WATTS, P. (1998), *Wavemaker Curves for Tsunamis Generated by Underwater Landslides*, J. Waterw. Port Coastal Ocean Eng. *124*, 127–137.

WIEGEL, R. L. (1955), *Laboratory Studies of Gravity Waves Generated by the Movement of a Submarine Body*, Trans. Am. Geophys. Union *36*, 759–774.

ZWILLINGER, D. (1989), *Handbook of Differential Equations*, Dept. Mathematical Sciences, Rensselaer Polytechnic Inst. Troy, New York, 379–382.

(Received September 9, 1999, accepted March 30, 2000)